Hydrological Processes

WILEY

RESEARCH ARTICLE

Insights Into Heterogeneous Streamflow Generation Processes and Water Contribution in Forested Headwaters

Jaime Ortega[1] | Catalina Segura[1] | J. Renée Brooks[2,3] | Pamela L. Sullivan[4]

[1]Department of Forest Engineering, Resources, and Management, Oregon State University, Corvallis, Oregon, USA | [2]Department of Forest Ecosystems and Society, Oregon State University, Corvallis, Oregon, USA | [3]Pacific Ecological Systems Division, Office of Research and Development, US Environmental Protection Agency, Corvallis, Oregon, USA | [4]College of Earth, Ocean, and Atmospheric Sciences, Oregon State University, Corvallis, Oregon, USA

Correspondence: Catalina Segura (segurac@oregonstate.edu)

Received: 13 October 2024 | **Revised:** 18 July 2025 | **Accepted:** 1 August 2025

Funding: This work was supported by National Science Foundation (EAR-1943574, EAR-2424997, EAR-2034232, EAR-2012796, LTER8DEB-2025755), SENACYT (Secretaría Nacional de Ciencia, Tecnología e Innovación) of Panamá.

Keywords: critical zone | damping ratios | end-member mixing analysis | isotopic lapse rates | storage | streamflow sources | water stable isotopes

ABSTRACT

Understanding how diverse headwater streams contribute water downstream is critical for accurate modelling of seasonal flow dynamics in larger systems. This study investigated how headwater catchments, with diverse subsurface storage, influence downstream flows within Lookout Creek—a 62 km^2, 5th-order catchment in the rain-snow transition zone in western Oregon, USA. We analysed one year of hydrometric and water stable isotope data collected at 10 stream locations, complemented by a decade of precipitation isotopic data. As expected, isotopic data revealed that most of the streamflow was sourced from large fall and winter storms. Generally, stream isotope ratios decrease with elevation. However, some streams had higher isotopic values than expected, reflecting the influence of isotopically heavy storms and relatively low storage. Other streams that tended to have low flow variability in response to precipitation inputs had lower isotopic values, indicating higher elevation water sources than their topographic watershed boundaries. Both hydrometric data and water isotope-based end-member mixing models suggest storage differences among headwater catchments influenced the seasonal water contributions from tributaries. Most notably, the contributions of Cold and Longer Creeks, which occupy less than 10% of the Lookout Creek drainage area, sustain up to 50% of the streamflow in the summer. These catchments have high storage and high groundwater contributions, as evidenced by flat flow duration curves. Finally, our data suggest that geologic variability and geomorphic complexity (presence of earthflows and landslides) can be indicators of storage that dramatically influence water movement through the critical zone, the variation in streamflow, and the response of streams to precipitation events. Heterogeneity in headwater catchment storage is key to understanding flow dynamics in mountainous regions and the response of streams to changes in climate and other disturbances.

1 | Introduction

Headwater mountainous systems play an important role in water quality (Alexander et al. 2007), aquatic biodiversity (Freeman et al. 2007; Meyer et al. 2007), and the downstream delivery of water (Birkel et al. 2020; Gomi et al. 2002). However, these systems are climatically diverse and physiographically complex, which complicates understanding what critical zone functions control local water flow path dynamics, streamflow generation processes, and their implications for downstream transport of water and solutes (Brantley et al. 2017; Lane et al. 2023). For example, understanding the impact of snowpack dynamics on streamflow generation will be critical in the face of the future climate impacts on streams near the rain-snow transition; yet

the response of mountain catchments to these dynamics will depend on their physiography.

The hydrologic regime in most mountainous temperate headwater streams is greatly controlled by elevation and the form and amount of precipitation, resulting in rain- and snow-dominated regimes (Moore and Wondzell 2005). Considering climate change predictions for the snowpack in many mountain ranges (Li et al. 2017; Mote et al. 2018; Siirila-Woodburn et al. 2021; Verfaillie et al. 2018), headwater streams in the current snow zone might ultimately become rain-dominated systems (Knowles et al. 2006). In many mountainous regions of the USA, this shift to rain-dominated precipitation could result in reduced streamflow (Berghuijs et al. 2014; Dierauer et al. 2018). These changes are expected to be non-uniform across the western U.S. (Hale et al. 2023) and influenced by elevation and subsurface storage (Barnhart et al. 2020; Vano et al. 2015) both of which can vary over very short distances.

Headwater streams often have a complex critical zone structure (Befus et al. 2011; St Clair et al. 2015), where storage variation among catchments can result in significant spatial differences in seasonal streamflow (Leuthold et al. 2021). As such, seasonal streamflow generation is strongly influenced by the underlying geology and geomorphic processes (Litwin et al. 2022) which control groundwater dynamics and subsurface storage (Segura et al. 2019; Thurber et al. 2024; Yao et al. 2021). The subsurface movement of water is influenced by features such as fractures (Fan et al. 2007; Johnson, Christensen, et al. 2024), the permeability of different lithologies (Nickolas et al. 2017), and the water storage capacity which is often modified by mass movement history (Segura et al. 2019). All these factors influence catchment storage, which includes dynamic storage—fraction that controls streamflow dynamics (sensu Staudinger et al. 2017)—and the often much larger passive (also call mobile) storage that can be inferred from tracers (Birkel et al. 2011; Soulsby et al. 2011). We suspect that the presence of geomorphic features will influence headwater catchment storage. However, we do not have a deep understanding of how geologic and geomorphic diversity across headwater catchments impacts and perhaps buffers downstream systems from climatological changes.

A useful approach for understanding streamflow contributions and storage within watersheds is the analysis of spatial and temporal variability of naturally occurring water stable isotopes (Bowen et al. 2019; Jasechko 2019). Water stable isotope ratios have been widely used to characterise precipitation inputs (Bowen and Revenaugh 2003; Bowen and Wilkinson 2002), catchment transit times (Benettin et al. 2022; McGuire and McDonnell 2006; McGuire et al. 2005; Segura 2021), and the origin of water sources within basins of different sizes (Brooks et al. 2012; Fennell et al. 2020; Jung et al. 2021; McGill et al. 2021; Nickolas et al. 2017; Segura et al. 2019; Windler et al. 2021). A key aspect of these studies was having detailed data on precipitation isotope ratios at the site to understand how these inputs have been modified and integrated over time within the catchment or basin (Clark and Fritz 1997; Putman et al. 2019). Precipitation isotope ratios vary both spatially and temporally, and depending on the system, can assist in understanding water origin and catchment storage properties. In general, the spatial variation in stream isotope ratios is influenced by the isotopic variation of precipitation inputs (Araguas-Araguas et al. 2000; Clark and Fritz 1997; Gat 2010). In mountainous regions, spatial variation in precipitation isotope ratios is generated by the rainout process and orographic lift, causing distinct lapse rates with elevation (Poage and Chamberlain 2001). Temporal variation of precipitation isotope ratios depends on the origin of vapour, temperature, and precipitation intensity, which varies with each precipitation event (Clark and Fritz 1997, Gat 2010). Temporal variation in stream water isotopes is generally driven by the temporal variation of precipitation inputs and the damping of that variation through internal mixing, and the rate of hydrologic cycling with more temporal variation with greater inputs, faster water movement, and less mixing (Bowen et al. 2019; Jasechko 2019). Both forms of isotopic variation can illuminate different aspects of catchment hydrology. Recent analytical schemes such as IsoSource (Phillips and Gregg 2003; Phillips et al. 2005) and Stable Isotope Analysis in R (Stock et al. 2018) allow estimating water contributions to complex mixing systems such as catchments when there are more than two end-members.

Here we explore how headwater catchments with diverse subsurface storage shift their contribution to downstream flows seasonally in a 5th-order catchment that spans rain and snow transition. We combined hydrometric and water isotopic ratios to investigate the spatial and temporal variability in water sources, runoff generation processes, and catchment storage. Specifically, we:

- Characterised the seasonal variability in water isotopic ratios in precipitation between water years 2015 and 2023 to understand how seasonal inputs to catchments might influence stream water stable isotopes across catchments with contrasting storage.
- Estimated tributary streamflow contributions to the downstream main stem over a year; inferred subsurface flow paths and storage variability using surface water isotope ratios and hydrometric metrics across tributaries and main stem locations.

Based on our results, we ultimately infer the spatiotemporal variability of subsurface flow paths and streamflow generation mechanisms to understand water source dynamics through the lenses of known differences in geology, geomorphology, and seasonal precipitation variability in headwater catchments.

2 | Methods

2.1 | Study Site

The study was conducted at the H.J. Andrews Experimental Forest (hereafter Lookout Creek), a Long-Term Ecological Research (LTER) site. Lookout Creek is a 5th-order stream that drains a 62 km^2 catchment in the Western Cascades of Oregon USA (Figure 1A). The catchment elevation varies from 411 to 1632 m (Figure 1B). The climate is Mediterranean with wet winters and dry summers and an average annual air temperature of 9.2°C (Daly et al. 2025) considering recent 20 years of data at the PRIMET meteorological station (430 m). During the sampling period (May 2022–May 2023), the monthly precipitation surpassed the 20 years long-term average, notably in May, June,

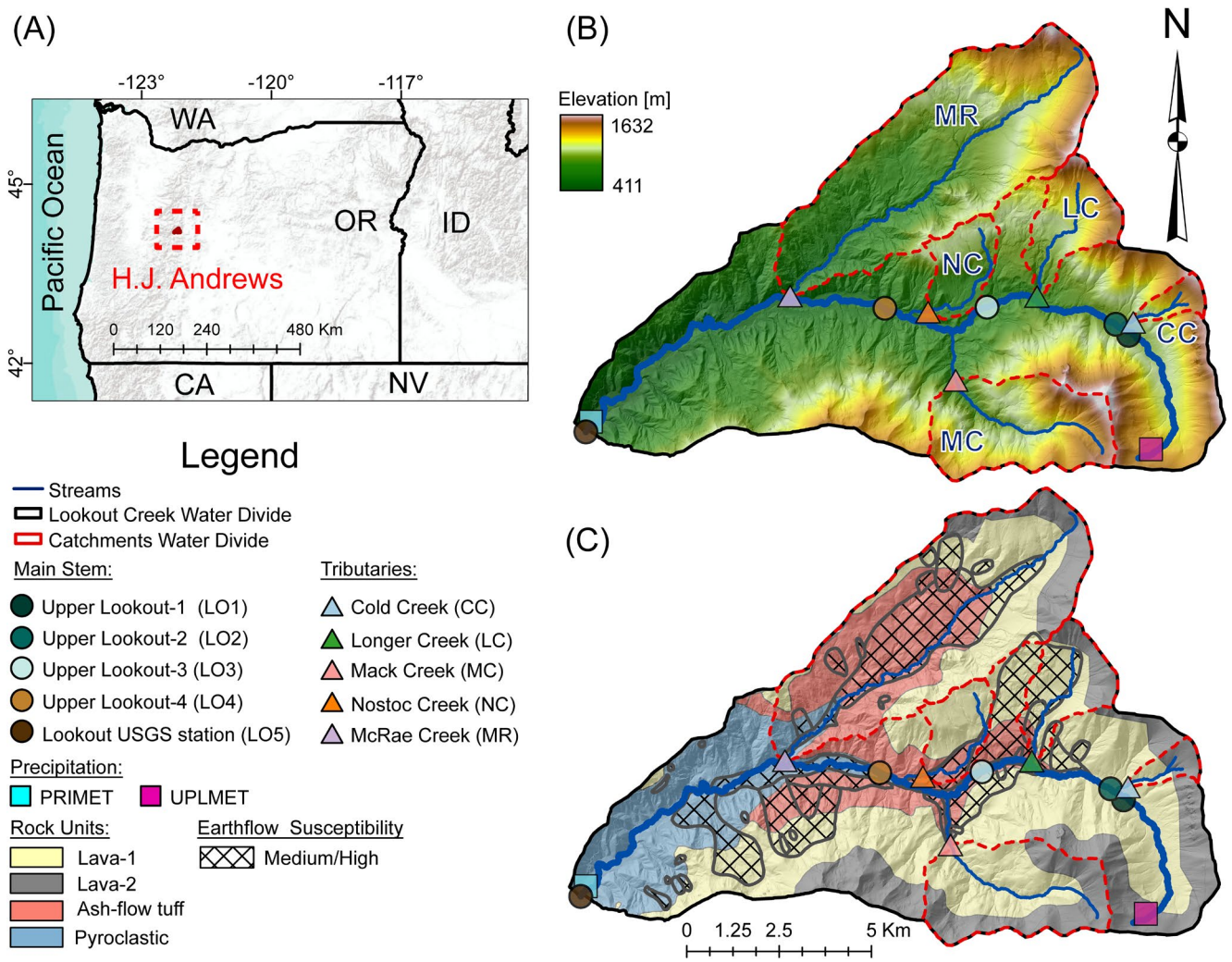

FIGURE 1 | (A) Location of the Lookout Creek catchment in Oregon. (B) Sampling sites across tributaries (△) and main stems (○) catchments in the Lookout Creek catchment. Tributaries are Cold Creek–CC, Longer Creek–LC, Mack Creek–MC, Nostoc Creek–NC, and McRae Creek–MR. (C) Geology (lithology) and earthflow susceptibility (medium and high) areas in the Lookout Creek catchment (Andrews Forest LTER Site and Swanson 2013; Swanson 2005).

and July 2022 (Figure S1). Conversely, April and May 2023 were lower than mean long-term values. The snowpack varies with elevation; for elevations between 400 and 800 m (transient snow zone), the snowpack persists for less than 2 weeks. Above 800 m (seasonal snow zone), the snowpack lasts up to 6 months, from November to June (Bierlmaier and McKee 1989). Snowpack at 1295 m (UPLMET) has varied in the last 20 years with maximum snow water equivalent (SWE) between 240 (in 2005) and 1570 mm (in 2023) (Daly et al. 2025; Ortega 2024). In 2015, Lookout Creek and surrounding areas experienced a severe snow drought (Segura 2021), while the SWE in 2017 (1270 mm) and 2023 (1570 mm) were above the median peak value (920 mm). Seasonal streamflow of Lookout Creek (USGS gauging station No. 14161500) reflects the transient snow (mixed rain-snow) influence with high flows in both winter (associated with rain events) and late spring (associated with snowmelt).

Lookout Creek is underlain by rocks of volcanic origin (Figure 1C) from the late Oligocene to early Miocene periods and exhibits three distinct zones: a region shaped by glacial activity, an area dominated by earthflows, and a zone characterised by debris slides and flows (Goodman et al. 2023). The glacially sculpted zone (Lava-1 and Lava-2), situated on resilient lava and ash-flow bedrock (Swanson and James 1975), features smooth terrain, cirques, truncated spur ridges, and U-shaped valleys, with minimal alteration by subsequent geomorphic processes. Cold, Mack, and a portion of Longer Creeks are located within this zone (Figure 1C). The earthflow-dominated area, developed on volcaniclastic formations of ash with significant shrink-swell clays capped by hard rocks (Swanson and James 1975), showcases notable landslide features, including earthflows. Nostoc, a portion of Longer, and McRae Creeks fall within this zone (Figure 1C). The debris-flow dominated region, formed on fragile volcaniclastic rocks (Swanson and James 1975), is characterised by rugged topography and steep slopes, primarily comprising the lower elevation area of Lookout Creek.

2.2 | Experimental Design

To explore how headwater systems contributed to mainstem flow, we selected five perennial tributaries with variable

drainage area and terrain characteristics (Figure 1B): Cold (CC), Longer (LC), Mack (MC), Nostoc (NC), and McRae (MR) Creeks, draining 0.69–15.6 km^2 with catchment mean elevations between 913 and 1297 m (Table 1). In addition, we sampled five sites along the main stem of Lookout Creek before and after the junction with some headwater tributaries and at the outlet with the USGS gauging station (LO1–LO5) with drainage areas between 5.5 and 62.4 km^2. These 10 sampling sites represent the diversity of catchments to Lookout Creek and were used to characterise their relative streamflow contribution (Table 1).

2.3 | Surface Water and Precipitation Sampling

Stream water samples were collected approximately weekly between May 2022 and May 2023, leading to a total of 277 samples across 10 sites (Table 1). Samples were collected from flowing water as close to the thalweg of the stream as possible. Sampling started in June 2022 at Nostoc, Longer, and Mack Creeks and in October 2020 at sites LO3 and LO4 (Table 1).

Composite precipitation samples have been collected weekly at the meteorological station PRIMET (430 m) since November 2014 using a Palmex Rain Sampler (Rain Sampler Palmex Ltd., Croatia) designed to limit evaporation (Groning et al. 2012). Snow was not frequent at PRIMET. On rare occasions (~4 per year), we found water frozen inside the sampler. In these cases, water in the sampler was thawed indoors before a liquid sample was collected. In total, 283 composite precipitation samples were collected between November 2014 and May 2023. Given restricted access to the study site during the 2019–2020 fire season, no precipitation samples were collected for 16 weeks between November 2018 and October 2019. To ensure that our annual and seasonal estimates of precipitation isotopes were not biased by this data gap, we estimated their isotope ratios based on the relationships between isotope ratios in Corvallis, OR (Brooks 2025) and isotope ratios in PRIMET. We found strong linear relations between overlapping samples collected between 2014 and 2023 that received over 10 mm of precipitation in Corvallis (Figures S2, S3). These relationships were also used to estimate isotope ratios for 1 week in 2015 and three weeks in 2017. Altogether, we included 317 composite precipitation samples in the analysis.

All water samples were collected in 20 mL borosilicate glass vials with conical inserts and capped without headspace to prevent evaporation. The samples were stored in dark and cool conditions (< 15°C) until they were analysed for water stable isotopes (Segura et al. 2024).

2.4 | Water Stable Isotopic Analysis

All water samples were analysed for stable isotope ratios ($\delta^{18}O$ and $\delta^{2}H$) using a Picarro L2130–I cavity ring down spectroscopy liquid and vapour isotopic analyser (Picarro Inc., CA). Samples were run under the high precision mode, with six injections per sample. The initial three injections were discarded to account for any memory effects (Qu et al. 2020). For calibration purposes we used two internal standards with $\delta^{18}O$ between −14.6‰ and −7.7‰ and $\delta^{2}H$ between −105.6‰ and −50.7‰. Additionally, a third internal standard ($\delta^{18}O$: −11.1 and $\delta^{2}H$: −80.1) was employed to estimate the accuracy of the analysis. All internal standards were calibrated with three of the International Atomic Energy Agency's primary standards: Vienna Standard Mean Ocean Water (VSMOW2), Greenland Ice Sheet Precipitation (GISP), and Standard Light Antarctic Precipitation (SLAP2). Precision (from 102 duplicated samples) was estimated as 0.02‰ for $\delta^{18}O$, 0.09‰ for $\delta^{2}H$, and 0.15‰ for deuterium excess (d-excess) (Brooks et al. 2022). The accuracy of the analyses was assessed by comparing 33 estimated values to a known internal standard, resulting in an accuracy of 0.01‰ ± 0.04‰ for $\delta^{18}O$ and 0.08‰ ± 0.25‰ for $\delta^{2}H$.

2.5 | Analytical Methods

2.5.1 | Streamflow and Specific Discharge Analysis

Streamflow records from 4 sites were used to investigate streamflow variability between May 2022 and May 2023. Two of these sites have long-term streamflow data: Lookout Creek-LO5 (USGS No. 14161500) and Mack Creek (Johnson, Wondzell, et al. 2024), while Cold and Longer Creeks were instrumented with pressure transducers (Solinst Canada Ltd.) to record 15-min stage. Discharge was measured using the velocity–area method (Dingman 2002) using either a FlowTracker (SonTek, Xylem Inc.) or a pigmy meter (Performance Results Plus Inc.), and depth-discharge rating curves were developed based on 5–9 discharge measurements per site (Ortega 2024) using a power-law function (Herschy 2009). To evaluate the hydrologic regime of the 4 streams, we estimated the flow duration curve (FDC) based on daily discharge records (England et al. 2018). Daily flows were normalised by drainage area for consistency (McMillan et al. 2017). The FDCs were used to infer flow variability (Buttle 2018). A relatively flat FDC is indicative of low flow variability that can be associated to high ground water contributions while a steep FDC indicates high flow variability and possibly low groundwater contributions (Safeeq and Hunsaker 2016; Sawicz et al. 2011). The drop in flow between the 5th and 95th percentiles (Q_5–Q_{95}) was used as a metric of flow variability (Buttle 2018). Finally, the monthly streamflow contribution from upstream gauged tributaries (Cold, Longer and Mack Creeks) to Lookout- LO5, $Q_{Partial}$ (%), was estimated:

$$Q_{Partial\,i} = \left(\frac{Q_{Tributary_i}}{Q_{Main\ stem}}\right) * 100 \quad (1)$$

where $Q_{Partial\,i}$ is the percentage (%) contribution of tributary to the main stem. $Q_{Tributary_i}$ is the discharge (m^3/s) of a given tributary, $Q_{Main\ stem}$ is the discharge (m^3/s) in Lookout Creek-LO5 and the subscript *i* correspond to the tributaries Cold, Longer, and Mack Creeks.

2.5.2 | Precipitation and Stream Isotopic Analysis

We calculated average, volume-weighted average (precipitation) and standard deviation for precipitation and stream isotope values. All data sets of $\delta^{18}O$, $\delta^{2}H$, and d-excess in precipitation and stream samples (Segura et al. 2024) were tested for normality. Differences across normally distributed data were tested using parametric tests including t-student (t test), analysis of variance (ANOVA), and Tukey test whereas differences across non-normally distributed data were performed

TABLE 1 | LiDAR derived topographic characteristics, lithology, mass movement presence, and available streamflow record of the study catchments: Cold Creek (CC), Longer Creek (LC), Mack Creek (MC), Nostoc Creek (NC), and McRae Creek (MR).

Catchment	DA (km²)	Max-Min Elev. (m)	CME (m)	CMS (°[%])	Coordinates (Lat°N/Lon°W)	Lithology[a] (%)	Mass movement[b] (%)	Available streamflow record	Sampling period
CC	0.69	1570–977	1297	27 [51]	44.229, −122.124	Lava-1 (58), Lava-2 (42)	Landslide (8)	2 (2021–2023)	May-22 to May-23
LC	2.74	1601–797	1178	23 [42]	44.234, −122.148	Lava-1 (64), Lava-2 (30), Ash (6)	Earthflow (46), Landslides (32)	1 (2022–2023)	Jun-22 to May-23
MC	5.75	1619–757	1197	28 [53]	44.219, −122.167	Lava-1 (55), Lava-2 (45)	Landslides (21)	28 (1996–2023)	May-22 to Feb-23
NC	1.96	1153–672	913	19 [34]	44.231, −122.174	Lava-1 (71), Ash (29)	Landslides (37), Earthflow (25)	—	Jun-22 to Feb-23
MR	15.58	1632–554	984	22 [40]	44.234, −122.208	Ash (46), Lava-1 (36), Lava-2 (13), Pyro (5)	Landslides (47), Earthflow (33)	—	May-22 to May-23
LO1	5.53	1620–927	1257	24 [44]	44.228, −122.127	Lava-1 (51), Lava-2 (49)	Landslides (3)	—	May-22 to Feb-23
LO2	6.32	1620–918	1258	25 [46]	44.229, −122.128	Lava-1 (51), Lava-2 (49)	Landslides (4)	—	May-22 to Feb-23
LO3	15.63	1620–723	1170	24 [44]	44.232, −122.160	Lava-1 (62), Lava-2 (31), Ash (7)	Earthflow (23), Landslides (22)	—	Oct-22 to May-23
LO4	30.67	1620–614	1106	25 [46]	44.232, −122.184	Lava-1 (60), Lava-2 (28), Ash (11), Pyro (1)	Landslides (28), Earthflow (17)	—	Oct-22 to May-23
LO5	62.42	1632–422	979	25 [46]	44.210, −122.257	Lava-1 (46), Lava-2 (18), Ash (21), Pyro (15)	Landslides (37), Earthflow (24)	74 (1950–2023)	May-22 to May-23

Note: LiDAR information obtained from Spies (2013). Coordinates represents the sampling point in each catchment. % represent the realtive area occupied by a given lithology and mass movemvent presence. LO1-LO5, are sites located in the main stem of Lookout Creek (Figure 1).

Abbreviations: CME, catchment mean elevation; CSE, catchment mean slope; DA, drainage area; Max-Min Elev, maximum and minimum elevation.

[a](Swanson 2005). Figure 1C.

[b](Swanson 2013). Figure 1C.

with the nonparametric Kruskal–Wallis test Kruskal (Kruskal and Wallis 1952) all in MATLAB (MathWorks Inc. 2023). Volume-weighted averages (precipitation) are indicated with a doubled overbar ($\overline{\overline{\delta^{18}O}}$ and $\overline{\overline{\delta^{2}H}}$) and the arithmetic average isotopic composition (streams) were presented with an overbar ($\overline{\delta^{18}O}$ and $\overline{\delta^{2}H}$), to distinguish them from individual isotopic samples ($\delta^{18}O$ and $\delta^{2}H$).

For precipitation data, we estimated volume-weighted Local Meteoric Water Lines (LMWL) on an annual and seasonal basis using the weekly $\delta^{18}O$ and $\delta^{2}H$ values collected at PRIMET between 2014 and 2023. LMWLs were based on a weighted least squares regression (Hughes and Crawford 2012) using Statsmodels package (Seabold and Perktold 2010) in Python considering 30–102 samples per season. The Global Meteoric Water Line GMWL ($\delta^{2}H = 8 \times \delta^{18}O + 10$) was considered for comparative purposes (Craig 1961). For this study, seasons were defined as: spring (20-Mar–20-Jun), summer (21-June–22-Sep), fall (23-Sep–20-Dec), and winter (21-Dec–19-Mar). Finally, we compared the annual and seasonal LMWLs to the Global Meteoric Water Line (GMWL) based on the analysis of covariance (ANCOVA).

For stream samples, we estimated isotopic lapse rates (relation between mean catchment elevation and mean isotopic ratios of stream water) using linear regression models (Beria et al. 2018; Poage and Chamberlain 2001).

2.5.3 | Damping Ratios

Isotope damping ratios (Bansah and Ali 2019; Kirchner et al. 2010; Sánchez-Murillo et al. 2015) were calculated for all investigated catchments. The damping ratio (DR) which has been previously assessed for two sites in Lookout Creek (McGuire et al. 2005) is the ratio of the standard deviation of stream (SD_{stream}) isotopic values to the standard deviation of precipitation isotopic values (SD_{Ppt}) for the same period of time:

$$DR = \frac{SD_{Stream}\left(\delta^{18}O \text{ or } \delta^{2}H\right)}{SD_{Ppt}\left(\delta^{18}O \text{ or } \delta^{2}H\right)} \quad (2)$$

2.5.4 | End-Member Mixing Analysis and Hydrograph Separation

Similarly to previous studies (Nickolas et al. 2017; Segura et al. 2019), we estimated the contribution of Cold, Longer, and McRae Creeks to Lookout Creek (LO5) based on a two-end member mixing model for each tracer ($\delta^{18}O$ and $\delta^{2}H$): With this approach we assumed that that inflow from groundwater along the mainstem is negligible.

$$Q_{down}C_{down} = Q_{up}C_{up} + Q_{trib}C_{trib} \quad (3)$$

$$F_{up} = \frac{C_{down} - C_{trib}}{C_{up} - C_{trib}} = \frac{Q_{up}}{Q_{down}} \quad (4)$$

$$F_{down} = \frac{C_{down} - C_{up}}{C_{trib} - C_{up}} = \frac{Q_{trib}}{Q_{down}} \quad (5)$$

$$F_{up} + F_{down} = 1 \quad (6)$$

where Q and C are streamflow and isotope ratios in upstream (up), tributary (trib), and downstream (down) locations in a network junction. F_{up} and F_{down} are the relative streamflow contributions from the upstream (up) flow and tributary (trib) to a downstream location (down).

The uncertainty in the two end-member model was propagated (Genereux 1998), and the error-weighted average of the fractional contribution obtained with both tracers is presented in the results. When there were more than two sources, we used the IsoSource Version 1.3 (Phillips and Gregg 2003) software, which provided a distribution of possible contributions for each end member. This strategy was used to estimate the contributions of LO3, Nostoc, and Mack Creeks to Lookout Creek (LO4). The uncertainty was estimated as the standard deviation of all possible solutions.

Two end-member mixing analysis using $\delta^{18}O$ was used to estimate event and pre-event water contributions for the largest precipitation event during the wet-up period in the fall of 2022 in all sites. This wet-up period started on 10-Oct-2022, ended on 11-Nov-2022, and delivered 337 mm in PRIMET (Figure 2). This fall precipitation started after an unusually dry period (i.e., precipitation in the month of September 2022 was below the 35 percentile considering data since 1980). The samples collected on November 5 in all streams increased to their highest observed isotopic values after a large precipitation event on November 4 that delivered 113 mm of precipitation, with isotope and discharge values increasing quickly between October 29 and November 11 (Figure 2). The volume-weighted average incoming precipitation (event water) for two samples collected between 26-Oct-2022 and 8-Nov-2022 was −9.5‰ for $\delta^{18}O$ and −62.4‰ for $\delta^{2}H$. We calculated the proportion of event water two ways: first, assuming the PRIMET value as the input, and second, we adjusted the input for varying elevation using an estimated stream lapse rate. We assumed that the mean isotopic values of stream samples collected ~8-Oct-2022–15-Oct-2022 represented pre-event water and that the event water at the peak stormflow was represented by samples collected in 5-Nov-2022. Using the two estimates, we propagated the error in the event and pre-event estimates (Genereux 1998).

3 | Results

3.1 | Hydrologic Regime and Streamflow Contributions

Precipitation during the study period (May 2022–May 2023) varied between 2155 mm in PRIMET and 2940 mm in UPMET and with the typical pattern for Lookout Creek with wet spring, dry summer, followed by large fall and winter storms (Figure 2 and Figure S1); fall 2022 was drier than typically observed, while winter snow inputs were large with peak SWE of 1570 mm. Average streamflow in Lookout Creek between May 2022 and May 2023 was 3.1 m^3/s, which was below the long-term annual average of 3.4 ± 0.1 m^3/s. Because of the large 2023 snowpack, spring (March–May) had over 21% more streamflow than the long-term values, while winter (December–February) had 47% lower streamflow compared to the seasonal long-term average (Figure S1). Streamflow at all sites reflected the seasonal

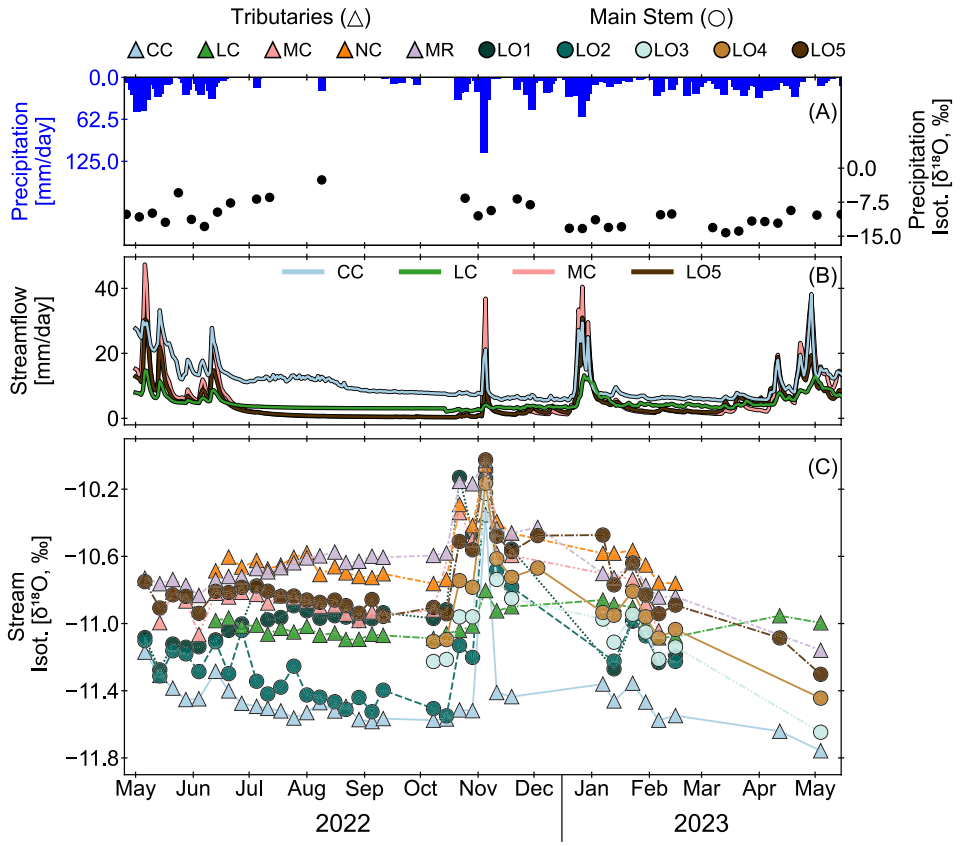

FIGURE 2 | Precipitation (mm/day), precipitation isotopic signature ($\delta^{18}O$), streamflow (mm/day), and stream isotopic signature ($\delta^{18}O$) during the study period (May 2022–May 2023) for the sampling sites (CC, LC, MC, NC, MR, and LO1–LO5).

variation in precipitation (Figure 2) and both streamflow and stream stable isotopic composition responded to the first large storm event in November (Figure 2).

The total specific discharge (streamflow divided by drainage area) ranged from 1735 mm in LO5 to 4206 mm in Cold Creek. Notoriously, during low flow conditions (July–October), Cold Creek had the highest specific discharge with values greater than 7.6 mm/day, followed by Longer Creek with unit area discharges higher than 2.7 mm/day (Figure 2, Table S1). Conversely, the specific discharge between July–October in Mack and LO5 was below 1.3 mm/day (Figure 2, Table S1).

High flows (Q_5) varied between 9.3 mm/day in Longer Creek and 23.5 mm/day in Cold Creek, while low flows (Q_{95}) ranged between 0.4 mm/day in Mack and LO5 and 5.8 mm/day in Cold Creek (Figure 3A and Table S2). The most dramatic Q_5–Q_{95} drop in flow occurred in Mack Creek, where flow decreased by 20.9 mm/day. The Q_5–Q_{95} drop in flow in Longer Creek was more stable over time, decreasing by only 6.4 mm/day (Table S2). The FDC slopes (Sawicz et al. 2011) were steeper in Mack (4.1) and LO5 (3.7) than in Cold (1.2) and Longer (1.1) Creeks (Table S2). The water contribution from high elevation catchments (Longer and Cold Creeks) to the outlet Lookout (LO5) was relatively large, reaching 51% in September (Figure 3B). The streamflow contribution from the tributaries (Cold, Mack and Longer Creeks) to LO5 ranged from 30% to 61% during periods of low

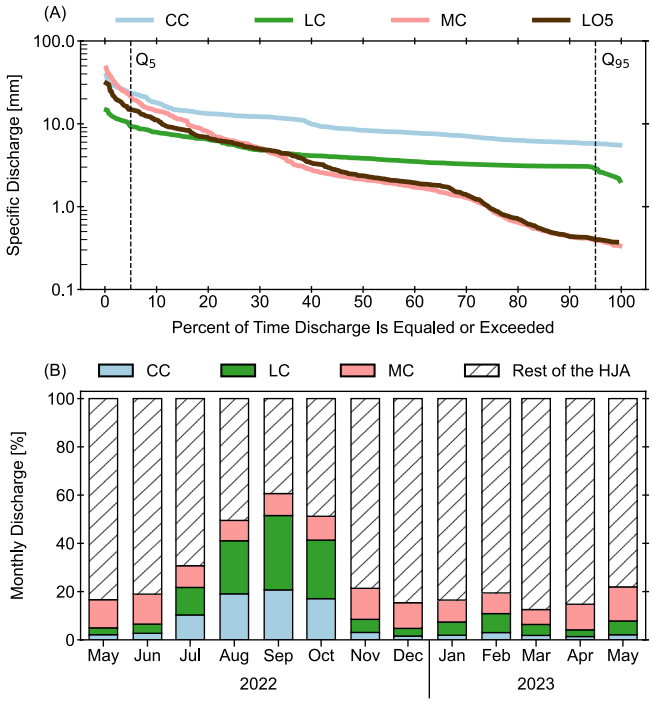

FIGURE 3 | Flow duration curve (A) for the gauged catchments and (B) relative monthly streamflow contribution (%) from Cold (CC), Longer (LC), and Mack (MC) Creeks to the Lookout Creek USGS station (LO5) during the sampling period (May 2022–May 2023).

flow conditions (July–October, Figure 3B). In contrast, throughout the remaining months (November–June), the proportional contribution for all these tributaries did not exceed 22%.

3.2 | Precipitation and Stream Isotopic Signatures

3.2.1 | Seasonal Variability of Precipitation Isotope Ratios

Weekly precipitation water isotope ratios 2015–2023 varied between −145.3‰ and −1.9‰ for δ^2H and −19.3‰ and 3.7‰ for $\delta^{18}O$ (Figure 4). The volume-weighted average precipitation isotopic ratios (2015–2023) for PRIMET were −72.2‰ ± 20.3‰ for $\overline{\overline{\delta^2H}}$, −10.4‰ ± 2.5‰ for $\overline{\overline{\delta^{18}O}}$, and 10.9‰ ± 4.4‰ for $\overline{\overline{d}}$-excess (Table S3). The volume-weighted average precipitation isotopic signature values for the sampling period (May 2022–May 2023) did not differ from the 2015–2023 (Table S3) values of $\delta^{18}O$, δ^2H, and d-excess (*t*-tests, $p = 0.09–0.66$).

Seasonally, the precipitation isotopic signature was strongly influenced by large fall and winter precipitation events associated with lighter values and high d-excess (Figure 4, S4A, Table S4). Conversely, precipitation events during the summer season were small and characterised by higher isotope values with low d-excess. Volume-weighted average isotope ratios for spring ($\overline{\overline{\delta^{18}O}}$: −10.4‰ ± 2.5‰) and winter ($\overline{\overline{\delta^{18}O}}$: −11.2‰ ± 2.4‰) were the lowest. In contrast, volume-weighted average isotope ratios in fall ($\overline{\overline{\delta^{18}O}}$: −9.5‰ ± 2.3‰) and summer ($\overline{\overline{\delta^{18}O}}$: −8.2‰ ± 2.4‰) were the highest (Table S4).

Precipitation d-excess varied significantly with seasons, with lower values in the spring ($\overline{\overline{d}}$-excess: 7.6‰ ± 4.7‰; $n = 95$) and summer ($\overline{\overline{d}}$-excess: 8.5‰ ± 7.6‰; $n = 30$) compared to the winter ($\overline{\overline{d}}$-excess: 11.4‰ ± 3.5‰; $n = 102$) and fall ($\overline{\overline{d}}$-excess: 13.0‰ ± 3.0‰; $n = 90$) (Table S4). Storms in the fall and winter were larger than in the spring and summer, with 55% of the weekly samples associated with over 50 mm of rain. In contrast, only 25% of the samples collected in the spring and summer were associated with precipitation amounts above 50 mm. Indeed, 61% of all precipitation between 2015 and 2023 had d-excess above 10‰, reflecting the relevance of fall and winter inputs (Figure S4).

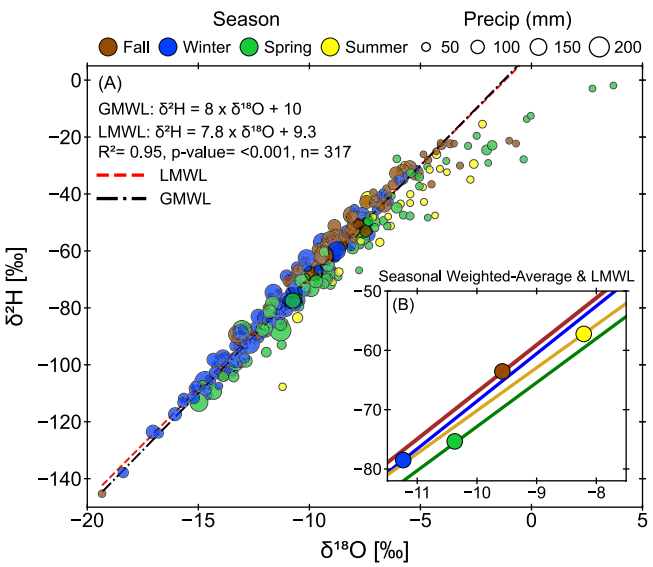

FIGURE 4 | Relationship between the $\delta^{18}O$ and δ^2H (A) values for the 317 weekly precipitation samples (November 2014–May 2023). All samples were included in the analysis. Red dashed line represents the Local Meteoric Water Line (LMWL) and the black dashed line represents the Global Water Meteoric Water Line (GMWL). The insert in the right-lower corner (B) includes the seasonal weighted isotopic values with their respective LMWL.

The seasonal differences in precipitation influenced the seasonal LMWLs, while the 2015–2023 LMWL was very similar to the GMWL. The slope of the LMWL for 2015–2023 (−7.8‰ ± 0.1‰) was not statistically different to the slope of the GMWL, although the intercept of 9.3‰ was significantly lower than the GMWL intercept of 10‰ (Table S5 and Figure 4). However, LMWLs differed seasonally; particularly, the seasonal LMWLs had significantly different intercepts, resulting in a series of parallel LMWLs (Figure 4B and Table S5). The spring LMWL had the lowest intercept with a low slope falling below the other seasonal LMWL (Figure 4B), followed by the summer LMWL. The fall and winter LMWL had significantly higher intercepts, with most precipitation values plotting above the 2015–2023 LMWL and GMWL. This significant seasonal difference in precipitation d-excess can be an excellent signal for distinguishing the seasonal origin of water within the stream (Sprenger et al. 2024).

3.2.2 | Seasonal and Spatial Variation in Water Isotopic Ratios in Stream Water

Water isotope ratios in the stream samples were less variable than in the precipitation samples (Figure 2). Isotope values across all stream samples varied from −80.7‰ to −67.3‰ for δ^2H, from −11.8‰ to −10.0‰ for $\delta^{18}O$, and from 10.2‰ to 14.6‰ for d-excess, with mean values of −74.5‰ ± 2.4‰ for δ^2H, −11.0‰ ± 0.3‰ for $\delta^{18}O$, and 13.2‰ ± 0.5‰ for $\overline{d}$-excess (Table 2). The isotope ratios in the tributaries were significantly less variable (i.e., lower standard deviation, Table 2) than the isotope ratios in the main stem (*t*-test, $p < 0.011$).

Seasonally, water isotopic ratios in streams were heavier in the fall than in all other seasons (Tables S6, S7). High isotope values systematically occurred in November during the first storm in 2023 (Figures 2 and 5). Conversely, in most sampling sites (6 out of 10), the lowest isotope values occurred in May. Mean seasonal stream d-excess was higher in spring ($\overline{d}$-excess: 13.4‰ ± 0.6‰) and winter ($\overline{d}$-excess: 13.3‰ ± 0.4‰) than in the summer ($\overline{d}$-excess: 13.1‰ ± 0.4‰) and fall ($\overline{d}$-excess: 13.0‰ ± 0.5‰, Tables S6, S7), but all were above the d-excess of the GMWL and LMWL.

Stream isotopic values varied spatially (Figure 6A). Among tributaries, Cold Creek, the most upstream catchment, had the lowest average isotopic signature ($\overline{\delta^{18}O}$: −11.4‰; $\overline{\delta^2H}$:-78.2‰, Table 2, Figures 2, 5). In contrast, Nostoc and McRae Creeks, the most downstream sampled tributaries, had the highest average isotopic signature ($\overline{\delta^{18}O}$: −10.6‰; $\overline{\delta^2H}$: −72.0‰, Figures 2 and 5). Within the main stem of Lookout Creek, the lowest average isotopic signature was in the second most upstream main

TABLE 2 | Summary of the mean and standard deviation (σ) for isotope ratios ($\overline{\delta^{18}O}$, $\overline{\delta^{2}H}$) and deuterium excess ($\overline{d}$) for stream samples collected at the different sampling sites.

Site	$\overline{\delta^{18}O} \pm \sigma$ (‰)	$\overline{\delta^{2}H} \pm \sigma$ (‰)	$\overline{d} \pm \sigma$ (‰)	Min ($\delta^{18}O$, $\delta^{2}H$, d)	Max ($\delta^{18}O$, $\delta^{2}H$, d)	n[a]
CC	−11.4 ± 0.2	−78.2 ± 1.7	13.4 ± 0.3	−11.8, −80.7, 12.7	−10.3, −69.6, 13.9	34
LC	−11.0 ± 0.1	−74.9 ± 0.6	13.1 ± 0.2	−11.0, −75.5, 12.6	−10.8, −73.2, 13.5	29
MC	−10.8 ± 0.2	−72.9 ± 1.6	13.6 ± 0.4	−11.2, −77.2, 10.2	−10.0, −67.5, 14.3	27
NC	−10.6 ± 0.2	−72.5 ± 1.2	12.3 ± 0.3	−11.5, −79.0, 12.9	−10.1, −67.7, 14.6	27
MR	−10.6 ± 0.2	−72.0 ± 1.5	13.1 ± 0.4	−11.6, −79.7, 12.7	−10.2, −68.3, 13.5	34
Average [Max, Min]	−10.9 ± 0.4	−74.2 ± 2.8	13.1 ± 0.5	[−11.8, −80.7, 11.4]	[−10.0, −67.3, 14.5]	151
LO1	−10.9 ± 0.3	−74.1 ± 2.0	13.2 ± 0.7	−11.4, −78.2, 12.6	−10.1, −68.0, 13.4	31
LO2	−11.2 ± 0.3	−76.3 ± 2.4	13.5 ± 0.3	−11.3, −77.0, 11.9	−10.0, −67.3, 14.0	31
LO3	−11.0 ± 0.3	−74.9 ± 2.5	13.3 ± 0.2	−11.0, −74.5, 12.7	−10.1, −67.5, 14.5	14
LO4	−10.9 ± 0.3	−73.8 ± 2.3	13.1 ± 0.2	−11.1, −75.9, 12.2	−10.0, −67.3, 14.2	15
LO5	−10.8 ± 0.2	−73.3 ± 1.7	13.0 ± 0.4	−10.7, −73.8, 11.4	−10.0, −68.2, 12.8	35
Average [Max, Min]	−11.0 ± 0.3	−74.5 ± 2.4	13.2 ± 0.5	[−11.6, −79.7, 10.2]	[−10.0, −67.3, 14.6]	126

[a]Number of samples.

stem catchment after the junction with Cold Creek (LO2, $\overline{\delta^{18}O}$: −11.2‰; $\delta^{2}H$: −76.3‰), while the most downstream location in Lookout Creek (LO5) had the highest average signature ($\overline{\delta^{18}O}$: −10.8‰; $\delta^{2}H$: −73.3‰) (Table 2, Figures 2 and 5). Finally, we also found that the standard deviation of the fall isotope ratios was significantly higher than the standard deviations in all other seasons (Tables S6, S7).

During the study period, a strong negative relationship between average surface water isotope ratios ($\overline{\delta^{18}O}$ and $\overline{\delta^{2}H}$) and catchment mean elevation (Figure 6B, Table S8) was evident. We found a positive relationship between d-excess and catchment elevation (R^2: 0.65, $p = 0.005$, Table S8). The isotopic lapse rates for the study period (considering average isotopic values per site) were −0.16‰/100 m for $\delta^{18}O$, −1.08‰/100 m for $\delta^{2}H$, and 0.21‰/100 m for $\overline{d}$-excess (Table S8). Despite these general trends, some catchments displayed different average isotope values than those expected solely based on catchment mean elevation. For example, even though the mean elevation of LO1 (1257 m) and LO2 (1258 m) were similar, the mean isotopic signature in LO1 was significantly higher (−10.9‰ for $\delta^{18}O$) than the mean isotope values in LO2 (−11.2 for $\delta^{18}O$) (ANOVA, $F = 36.5–39.6$ for $\delta^{18}O$ and $\delta^{2}H$, Tukey test, $p < 8.0\ 10^{-5}$).

3.2.3 | Damping Ratios

The damping ratio indicates stream isotopic variation relative to the precipitation isotopic variation. Since the same value of precipitation isotope variation was used for all streams in the study, variation in this ratio indicated differences in stream variance. The $\delta^{18}O$ and $\delta^{2}H$ damping ratios varied between 0.03 (Longer Creek) and 0.14 (LO1). Broadly, damping ratios were lower across tributaries than across the main stem sites (Figure S5A) and were moderately correlated ($R^2 = 0.80$, $p = 0.1$) to the $Q_5–Q_{95}$ drop in flow for the four catchments with streamflow data. Across the five tributaries, the average damping ratio was 0.08 for both $\delta^{18}O$ and $\delta^{2}H$. Mack Creek (0.10) and McRae (0.09) Creeks had the highest damping ratios for both isotope ratios, whereas Longer Creer had the lowest damping ratio (0.03). Across the five main stem sampling sites, the average damping ratio was 0.13 for both $\delta^{18}O$ and $\delta^{2}H$. LO3 had the highest value with 0.15, while LO5 had the lowest ratio (0.10) (Figure S5A). The damping ratio at the outlet of Lookout Creek (LO5) overlaps the damping ratios for McRae and Mack Creeks reflecting the large influence of the largest tributaries (by drainage area, Table 1). The damping ratios in Nostoc and Longer Creeks were the lowest, implying that these systems potentially drain water that has been in storage for a longer time. While Cold Creek also had a relatively high damping ratio (high variance), this higher variance was driven by the high isotope value measured after the largest precipitation event in Nov 2022 (Figures 2 and 5). Without this one event, the damping ratio in Cold Creek would have been 55% lower (0.04). The damping ratios for all other sites were influenced by this precipitation event to a lesser degree (Figure S5B).

3.2.4 | Linking Precipitation and Stream Isotopic Signature Patterns

Stream dual isotope plots showed that streamflow isotope values varied seasonally and consistently exhibited higher d-excess compared to precipitation (Figure 5). In general, stream isotope ratios were elevated during the summer and fall, particularly during the first large storm event in November (Figures 2 and 5). The relationships between $\delta^{18}O$ and $\delta^{2}H$ were strong, with slopes ranging from 6.5 to 8.1, showing less variation than the intercepts, which ranged from −3.5‰ to 14.1‰ (Figure 5). In all cases, stream isotope ratios plotted

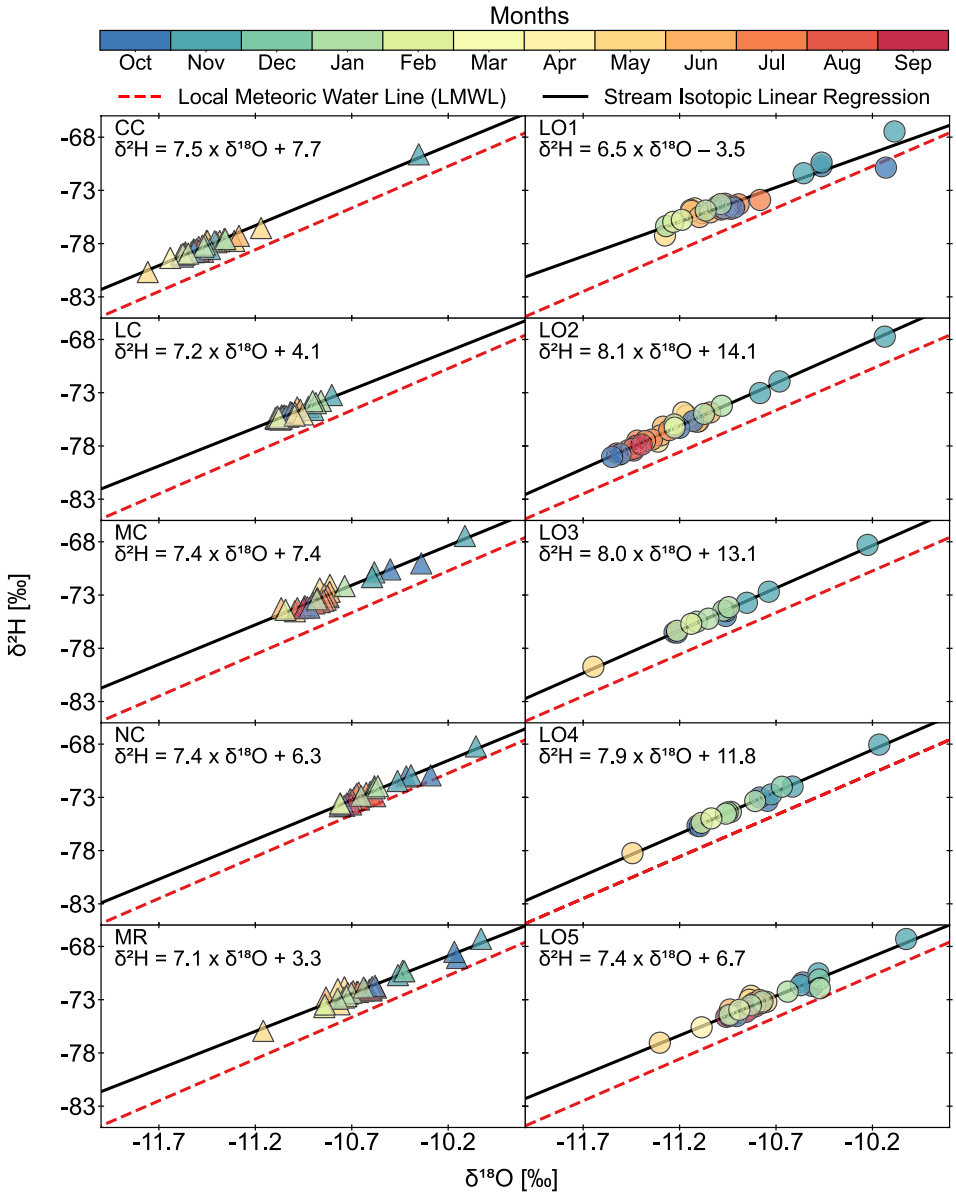

FIGURE 5 | Dual isotope plot ($\overline{\delta^{18}O}$ and $\overline{\delta^{2}H}$) by catchment. A linear regression line (black line) was estimated using the isotopic signature of each site. The Local Meteoric Water line (LMWL) from PRIMET for the May 2022—May 2023 period, was also included for reference (red dashed line). Left column includes tributaries: Cold (CC), Longer (LC), Mack (MC), Nostoc (NC), and McRae (MR) Creeks. The right column includes the main stem sampling locations in Lookout Creek (LO1–LO5). Points are coloured to indicate the month in which each sample was collected.

systematically above the mean local meteoric water line, regardless of season (Figure 5).

Assessing the location of seasonal average stream isotopic signatures in the dual isotope plots (Figure 7) provides insights into the seasonal influence of meteoric water on streamflow. During the fall season, water isotope ratios in the streams plotted along the fall LMWL, but well above the GMWL and 2015–2023 LMWL (Figure 7A). In contrast, stream water isotope ratios from other seasons plotted well above their seasonal LMWL, the GMWL and 2015–2023 LMWL (Figure 7B–D), stream water isotope values from all seasons matched that of the fall LMWL. The seasonal average d-excess values for stream samples across sampling sites were similar (12.1‰–13.8‰) to the seasonal weighted average d-excess in precipitation samples collected in the fall (13‰) and winter (11.4‰); however, they were greater than the weighted average precipitation d-excess in the spring (7.6‰) and summer (8.5‰) (Figure S6).

3.3 | End-Member Mixing Analysis and Hydrograph Separation

3.3.1 | Tributary Streamflow Contributions

End-member mixing analysis with both $\overline{\delta^{18}O}$ and $\overline{\delta^{2}H}$ was used to estimate the streamflow contribution of the sampled tributaries to Lookout Creek and the uncertainties (Figure 8). Seasonal dynamics in streamflow contribution were evident at the most upstream junction of LO1 and Cold Creek into LO2, where we had the most data. Cold Creek contributed most of the flow (70% to 90%) to LO2 during low flow conditions

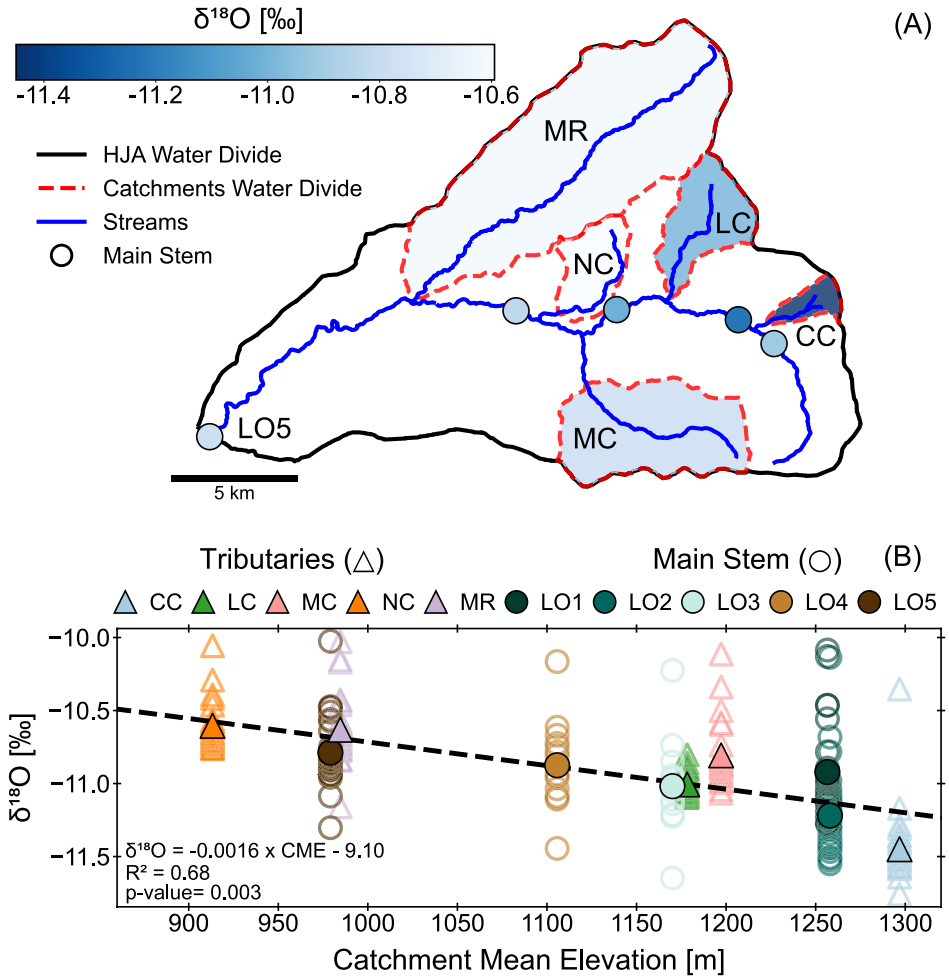

FIGURE 6 | Spatial distribution of the average stream isotopic signature ($\overline{\delta^{18}O}$) represented by blue shading across sampling sites in Lookout Creek (coloured circles) and tributaries (shaded catchments) between May 2022 and May 2023 (A). Red and black water divide represent headwater streams and Lookout Creek boundary. (B) Relationship between mean catchment elevation and stream average isotopic signature ($\delta^{18}O$) by catchment. Filled and unfilled markers depict the average and individual sample values. Linear regression line (dashed black line) was estimated using the average isotopic signature of each sampled site.

(July–October) (Figure 8B,C), even though Cold Creek comprises only 11% of the catchment area for LO2. In contrast, during wetter periods, LO1 contributed the most flow to LO2. In May, June, November, January, and February, the LO1 contribution to LO2 varied from 65% to 100%. For other stream junctions water contributions could only be determined for 4 months (October, November, January, and February). Longer Creek supplied more to LO3 than LO2 in October, contributing 93% of the flow (Figure 8B,C) while being only 18% of the catchment area for LO3. In November, January, and February when discharge was higher, LO2 contributed over 65% of the water downstream to LO3 which was more representative of its proportion of the catchment (Figure 8B,C). Nostoc and Mack Creeks never contributed more than LO3 to flow in LO4 with average contributions of 14% for Nostoc (6.4% of the LO4 catchment) and 29% for Mack (19% of the LO4 catchment). The streamflow contribution of LO3 was consistently above 60% (Figure 8B,C). Finally, the streamflow contributions to LO5 were predominantly from McRae Creek, averaging 68%. October was the only month when Upper-Lookout Creek 4 (LO4) contributed more discharge than McRae Creek, with a contribution of 65% (Figure 8B,C).

3.3.2 | Storm Hydrograph Separation

Using $\delta^{18}O$ values in stream and precipitation samples, we estimated the relative contribution of event and pre-event water for the wet-up precipitation in the fall of 2022 that evoked a hydrologic response. The mean weighted pre-event water contribution varied between 31% and 49% for Cold, Mack, Nostoc, and McRae Creeks; and 29% and 61% for all LO1–LO5 and over 80% for Longer Creek, while discharge increased nearly two orders of magnitude at LO5 (Table S9). Hydrometric analysis (Table 1) indicated that peak streamflow occurred on 04-Nov-2022 (Cold Creek and Longer Creek) and on 05-Nov-2022 (Mack Creek and LO5) (Table S9).

4 | Discussion

We found that flow in a 5th-order mountainous stream depended on a range of short- to long-term water storage mechanisms. Five headwater streams varied in their damping ratios, indicating a range of water storage and groundwater connectivity, resulting in temporally variable contributions for each headwater

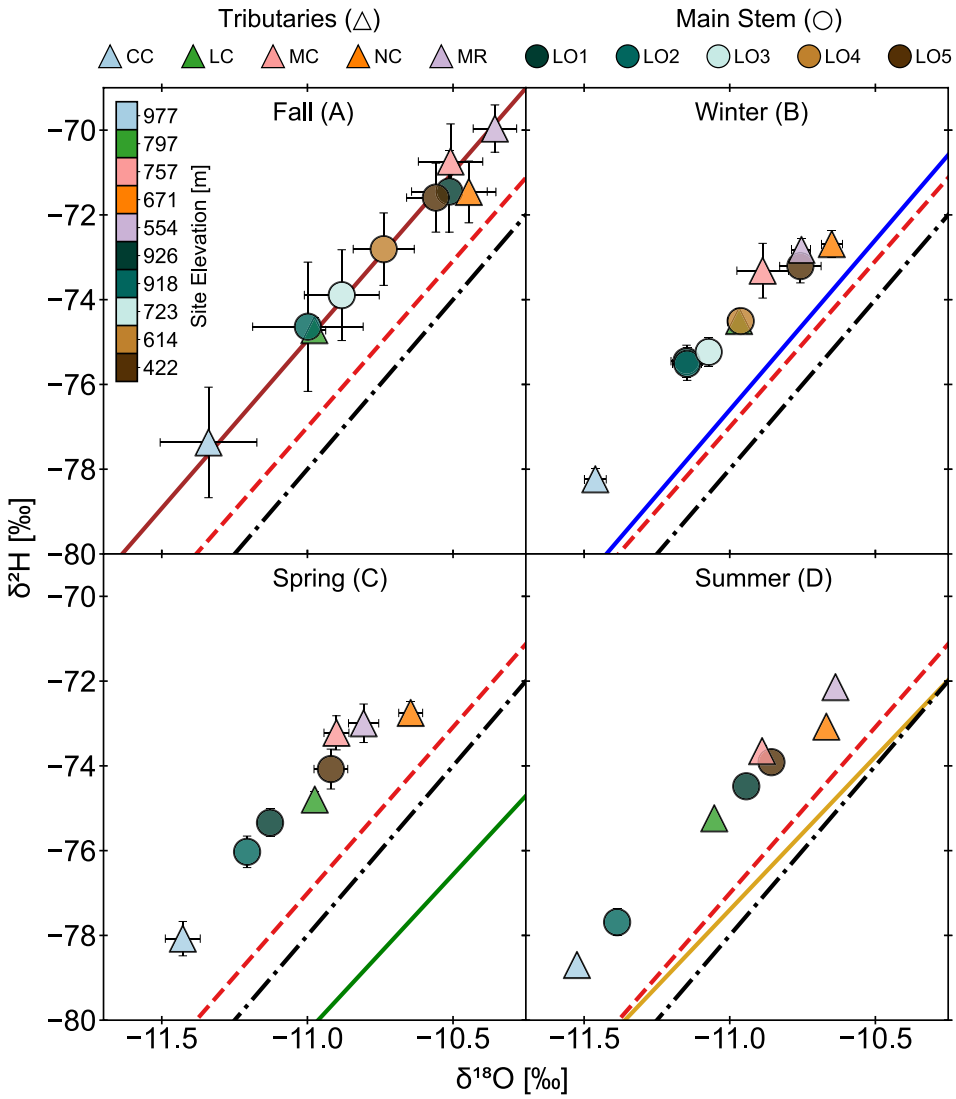

FIGURE 7 | Seasonal (A–D) dual stream isotopic plot across all study catchments between 2015 and 2023. Black dashed line is the global meteoric water line (GMWL), and the seasonal local meteoric water lines (LMWL) are in solid colours. The 2015–2023 LMWL is included (red-dashed line). Error bars are standard errors. Seasons were defined: Spring (03/20–06/20), summer (06/21–09/22), fall (09/23–12/20), and winter (12/21–03/19).

catchment to downstream flow. This variability among tributaries likely contributes to the maintenance of flow at the downstream gauging station (LO5) where a few headwater streams with low damping ratios and dampen flow duration curves (FDC) provide most of the flow during low flow periods, while headwater systems with higher damping ratios and steeper FDC contribute most flow during the wetter period. Observations during the first large precipitation event (Figure 2), after a relatively dry fall, indicated that pre-event water contributions were in part controlled by differences in storage inferred from earthflow and landslides terrain. We found higher fractions of pre-event water in catchments with a high presence of these depositions. We speculate that the storage capacity of these deposits enhances connectivity between surface and groundwater sources. We found that water isotopes in streamflow reflected precipitation isotopes with high d-excess values, only matching the fall local meteoric water line (LMWL). This indicates that large fall and early winter storms with high d-excess (Figure S4B) preferentially recharged water storage that then supplied streamflow year-round to these systems.

4.1 | Seasonal Precipitation Influence on Streamflow Sources

Seasonal isotopic differences, particularly in d-excess, proved to be a useful tool for understanding the seasonal origin of water within the stream network. Seasonal LMWL at the Lookout Creek catchment had similar slopes to the GMWL and the long-term (2015–2023) LMWL in all seasons except for spring, which was significantly less steep. Conversely, the intercept of the LMWLs varied widely and was, in all cases, different. The intercept of the LMWL in spring (1.4‰) and summer (2.1‰) is much lower than the intercept for the GMWL (10‰) while the intercept for the fall (11.9‰) and winter (11.6‰) is much higher than 10‰. The difference for spring and summer could be attributed to kinetic fractionation during the evaporation of rain droplets (precipitation subject to secondary evaporation) below the cloud base, which can result in a slope lower than 8‰ (Dogramaci et al. 2012; Gat and Matsui 1991; Martinelli et al. 1996). Frontal systems during the spring and summer are likely strongly influenced

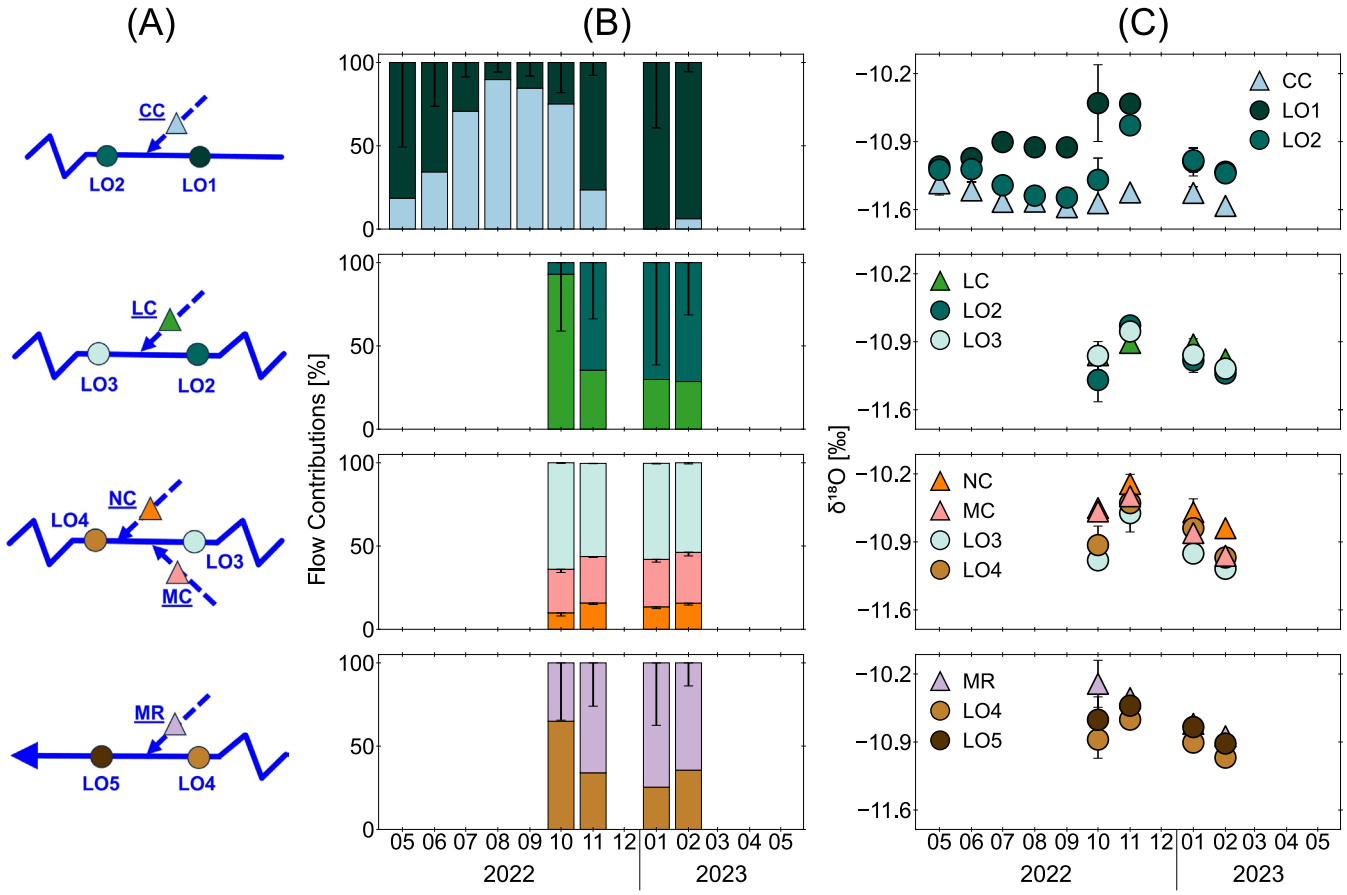

FIGURE 8 | Streamflow contribution to Lookout Creek from Cold, (CC), Longer (LC), Nostoc (NC), Mack (MC), and McRae (MR) Creeks. Stream diagram (A) illustrates the layout of end-members and outlets along the Lookout Creek. (B) shows the monthly streamflow contribution from the tributaries in (A) and associated uncertainty (black lines at the top of the bars), and water stable isotope ratios (C) represents stream average isotopic signature in tributaries and main stem, with error bars denoting the standard deviation. In (B), for the mixing models with two 2 end-members, the error bars indicate weighted standard deviation (error propagation), considering $\delta^{18}O$ and $\delta^{2}H$. For the group with 3 end-members (MC, NC, LO3) the error bars represent the standard deviation of the distributions of possible solutions obtained with IsoSource. No samples were collected in LO3 and LO4 between May and Sep 2022 thus no estimates of streamflow contributions from LC, NC, MC or MR were possible.

by nonequilibrium evaporation at the source due to frequent high temperatures during relatively smaller storm magnitudes (Benjamin et al. 2005; Jeelani et al. 2013). This is consistent with observations in arid (Clark and Fritz 1997; Kendall and Coplen 2001) and humid regions during dry springs and summers (Müller et al. 2017; Nickolas et al. 2017).

The intercept of the LMWL in the fall and winter was significantly higher than the intercept of the GMWL, indicating the influence of high d-excess vapour sources that formed at relatively low temperature and relative humidity with mixed ice-rain phase clouds (Putman et al. 2019). Putman et al. (2019) found that precipitation d-excess was often much higher during cold seasons as compared to warm seasons at the same site. In Lookout Creek, precipitation with d-excess above 10‰ occurred primarily in the fall and winter, corresponding to almost two-thirds of all water inputs between 2015 and 2023 (Figure S4B).

Unlike precipitation inputs, stream isotopic ratios had consistently high d-excess of approximately 13.2‰ (Figure S6) and varied seasonally along a single dual isotope line that was above the LMWL (Figure 5). The high d-excess value highlighted the importance of fall and winter storms as the dominant water source for streams year round (Sprenger et al. 2024). This is not surprising considering that most precipitation is received during these seasons (Bierlmaier and McKee 1989; Crampe et al. 2021; Jones and Perkins 2010), and plant transpiration is relatively low. In contrast, spring and summer precipitation inputs appear to have had less influence on stream waters. Despite high soil moisture storage, summer inputs to streamflow would be expected to be negligible considering the low precipitation volumes (Figure 4 and Figure S1) and the competing demand from plant transpiration. While spring inputs are larger, plant transpiration is likely larger in spring than in fall and winter (Perry and Jones 2017). In addition, snowmelt, which reflects stored winter precipitation, would also dampen the signal from spring storms (Jennings and Jones 2015). The winter of 2023 had a relatively large snowpack, and when snowmelt entered the streams in May, we observed the lowest isotope ratios (Figures 2 and 5) which were much lower than isotope ratios from the incoming precipitation at the time.

As observed across many mountain ranges, mean isotopic values decreased with catchment elevation (e.g., Bershaw et al. 2016;

Peng et al. 2015; Wassenaar et al. 2011), which we assume is driven by the rain-out process with precipitation and orographic lift. However, we had only one location for precipitation isotope values, so our inferences in this spatial variation are made from surface water measurements. Our calculated surface water elevation lapse rates (1.61‰ km^{-1} for $\delta^{18}O$ and 10.7‰ km^{-1} for $\delta^{2}H$) were similar to a precipitation lapse rate calculated for the same site (0.15‰ km^{-1} for $\delta^{18}O$) (McGuire et al. 2005) and to the mean lapse rates calculated for high-elevation springs in the Cascade mountains (1.6‰ $km^{-1}$for $\delta^{18}O$ and 10.57‰ $km^{-1}$for $\delta^{2}H$) (Jefferson et al. 2006) and smaller than a surface water lapse rate calculated for the larger Cascade Mountain region (2.8‰ km −1 for $\delta^{18}O$ and 20.6‰ km −1 for δ^{2} H) (Brooks et al. 2012). The positive relation we found between mean catchment elevation and d-excess was previously reported for the summer at this site (Segura et al. 2019) and for other mountainous regions (Bershaw et al. 2012; McGill et al. 2021; Voss et al. 2020). This relation could reflect greater Rayleigh distillation and moisture recycling in lower elevations and the larger contribution of snow with elevation (Ciais and Jouzel 1994; Putman et al. 2019; Sprenger et al. 2024).

4.2 | Influence of Headwater Catchment Heterogeneity on Streamflow Generation

Although the relationship between the isotopic composition of stream water and elevation is strong, there were considerable deviations from the linear fit (Figure 6B), especially LO1, Mack, and Cold Creeks. The lighter water in Cold Creek has been reported before for the summer (Segura et al. 2019) and reflects an important high elevation water source (Bershaw et al. 2012; Gonfiantini et al. 2001; Liotta et al. 2013). In contrast, Mack Creek and LO1 were characterised by mean isotopic signatures that were higher than expected (Figure 6B) likely reflecting a stronger relative influence of precipitation events and lower subsurface storage. Although the mean isotope values for the remaining seven locations varied consistently with the estimated lapse rate, the variance of isotope ratios within catchments was different among sites. Isotope ratios within tributaries were less variable than isotope ratios within the main stem sites. The higher variability in the isotope ratios for the main stem sites is caused by the temporally changing contributions from upstream catchments and, at least in part, the influence of the inputs from intermittent streams that seasonally drain water during the wet seasons in this region. As such, the standard deviation of the isotope ratios collected during the fall was higher than the standard deviations for samples collected in all other seasons (Tables S6, S7). This variable input from upstream catchments to downstream flow seasonally buffers to some degree the temporal variation of precipitation inputs as short- to long-term storage pools were filled and emptied at different rates through time (Leibowitz et al. 2016; Spence 2007). Among tributaries, isotopic variability in Longer Creek was much lower than the isotopic variability of any other site, indicating that this has a large stable subsurface storage that remains connected to streamflow and, as such, was affected the least by discrete storms.

The relatively lower FDC slope for Longer and Cold Creeks compared to other streams (Figure 3) can be interpreted as indicative of relatively high groundwater contributions. Differences in storage were also reflected in the variability of water isotope ratios. Isotope ratios in McRae and Mack Creeks and LO1 were much more variable than in Cold and Longer Creeks, reflecting lower storage. Streamflow in these streams is likely more responsive to variations in precipitation (Huang and Yeh 2022) as inferred from the higher FDC slope for Mack compared to Cold and Longer Creeks (Table S2). This variability among catchments reflected differences in storage that were exacerbated during dry summer conditions and influenced their seasonal contributions to downstream sites.

4.3 | Variable Storage Influence Streamflow Generation and Water Contributions

The role of groundwater in streamflow generation has been a subject of debate. Early studies highlighted its relevance as a major component of storm flow (e.g., Maloszewski et al. 1983; Sklash and Farvolden 1979). Later, some suggested that groundwater actually plays a minimal role in streamflow generation in mountain systems due to steep slopes and shallow soil development (McGlynn et al. 2002; Weiler et al. 2006). However, recent research has shown that mountain catchments can have a substantial capacity for groundwater storage and discharge, which is crucial for maintaining streamflow during dry periods in mountains in the Andes (Calvi et al. 2024), California (Johnson et al. 2023), Colorado (Johnson, Christensen, et al. 2024; Johnson et al. 2025), Germany (Uhlenbrook et al. 2002), Oregon (Karlstrom et al. 2025), Scotland (Soulsby et al. 2000), and Spain (Jódar et al. 2017). Here, we rely on metrics of flow variability and groundwater influence derived from hydrometric information such as the Q_5–Q_{95} drop in flow (Buttle 2018), the slope of the FDC (Sawicz et al. 2011) and metrics of mobile storage—isotope derived damping ratios (e.g., Kirchner et al. 2010; McGuire et al. 2005; Soulsby et al. 2015). In addition, we considered the presence of geomorphic features such as earthflows and landslide deposits to infer spatial variability of storage potential (Segura et al. 2019; Somers and McKenzie 2020).

The observed variability in Q_5–Q_{95} drop in flow, the FDC slope, and the isotope damping ratios highlights heterogeneity in runoff generation. Cold and Longer Creeks exhibit lower slopes in the FDC than Mack Creek (Figure 3, Table S2), suggesting greater groundwater contribution. The spatial variability in damping ratios is partially explained by the presence of geomorphic features with landslide and earthflow deposits linked to lower damping ratios and higher mobile storage (Figure 9A) (McGuire et al. 2005; Swanson and James 1975). Longer and Nostoc Creeks, with over 60% of their drainage areas underlain by these features, have low damping ratios (Figure 9).

Lower isotope variability in Longer Creek aligns with its low Q_5–Q_{95} drop (i.e., low FDC slope), indicating a well-mixed groundwater source (McGuire and McDonnell 2006; Soulsby et al. 2006). While McRae and Longer Creeks have similar catchment slopes and earthflow and landslide coverage (Table 1), McRae's higher damping ratio suggests lower mobile storage, possibly due to differences in deposit porosity. McRae Creek drains more incised streams over landslides of different ages, whereas Longer Creek, in glaciated terrain, has active earthflows and twice as much permeable young lava flows (Goodman et al. 2023; Swanson and

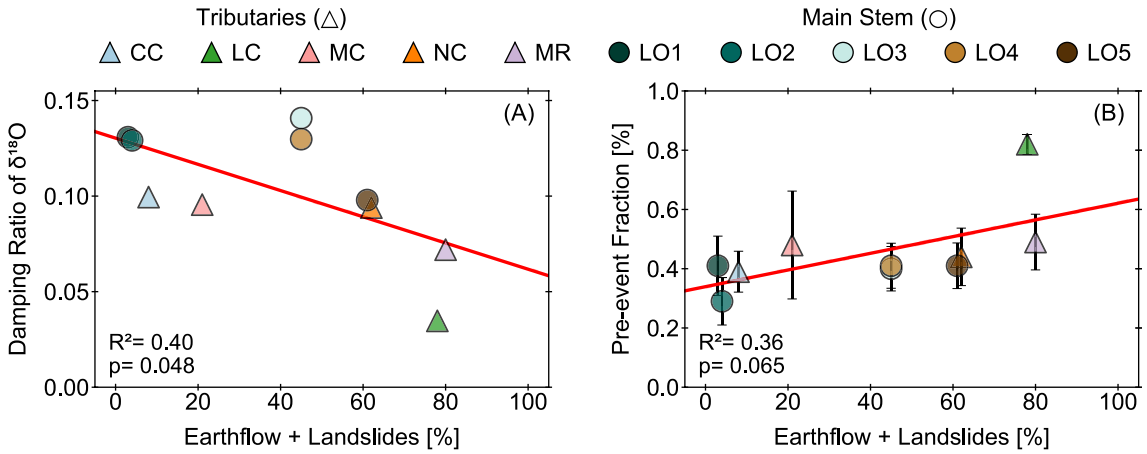

FIGURE 9 | Relationship between the damping ratio ($\delta^{18}O$) (A) and the pre-event water fraction of the November 2022 storm event in the study catchments, in relation to geomorphic features: Earthflows and landslides. The error bars in (B) represent the weighted error considering two different event water estimates (Table S9).

James 1975). These porous deposits enhance storage, explaining why catchments like Longer and Cold Creeks sustain significant streamflow during dry conditions (Karlstrom et al. 2025; Segura et al. 2019).

Specific discharge in August–October 2022 in Cold and Longer Creeks was 16–18 and 5–7 times higher than in Lookout Creek (Table S1). Studies have highlighted the controlling effect of moisture availability and evapotranspiration (Lyon et al. 2012), geology, and topography (Asano et al. 2020) on specific discharge with no clear consensus across variability or drivers (Floriancic et al. 2019). During the low flow period, Cold and Longer Creeks support ~50% of the total flow in Lookout. Water isotope ratios in Cold Creek were the lowest (Figure 2). Notably, lower than in LO1 located at similar elevation (Table 1). Given the high specific discharge, the low isotopic ratios, and the relatively high water contribution of this stream to Lookout Creek, we infer that Cold Creek is sourced in part from a large groundwater storage recharge through the permeable lava flows that underlain 40% of its drainage and are located in the catchment ridge (Figure 1). Given Cold Creek's limited drainage area and the consistently low stable isotope ratios throughout the year, local snowmelt alone cannot account for the observed groundwater input. It is more likely that most recharge occurs during the wet season from precipitation falling outside the catchment's topographic boundaries, particularly along the ridge overlying the lava flows (Karlstrom et al. 2025, Segura et al. 2019). This mechanism is also possible in Longer Creek but to a lesser extent, not only because the specific discharge in Longer Creek was not as high as in Cold Creek but also because the lower isotopic variability implies a well-mixed local water source. Together, the information from the flow duration curve, damping ratios, and the presence of geomorphic features indicated that Cold and Longer Creeks have higher contributions of groundwater compared to the other catchments. These streams supply substantial amounts of water during the summer and are critical sources of water for Lookout Creek.

The wet-up period we analysed corresponded to the first hydrograph response in the 2023 water year after a very long dry period. The hydrograph separation results illustrate differences in pre-event water contributions that are in part controlled by differences in storage. Catchments with high earthflow and landslide fractions had higher pre-event water. The pre-event fraction was below 50% across sites except Longer Creek, which had a pre-event fraction > 82% (Figure 9B). This indicates that storage and groundwater contributions in this site are large and mobilised to the stream even during dry conditions, whereas the contribution of groundwater in Cold Creek during the storm appears to be much smaller, with only 39% of pre-event fraction. The unexpectedly high damping ratio for Cold Creek (Figure S3A) was mainly driven by one high isotopic value collected during the precipitation event (Figure 2). Without this one sample, Cold Creek had a damping ratio similar to Longer and Nostoc Creeks (Figure S5B). This indicates that during this first storm a large fraction of the water in Cold Creek was possibly sourced from the event precipitation and not from groundwater. Likely, connectivity between the stream and the high elevation sourced groundwater was low during this unusual dry fall period. Although the storm delivered a significant amount of event water to Cold Creek, the increased moisture appeared to have quickly promoted the reconnection of Cold Creek to its isotopically lighter groundwater source, as stream isotope values quickly returned to the pre-event values (Figure 2).

4.4 | Implications

The variable hydrologic response observed in small catchments is fundamental to understanding streamflow variability at the outlet. In the context of mountainous catchments, outlet-based observations alone are insufficient to capture the spatially heterogeneous responses of different catchment components to changing hydrometeorological conditions (Floriancic et al. 2019). These findings have significant implications for hydrological modelling and scaling, as they highlight the necessity of incorporating spatial variability in runoff generation processes. The observed heterogeneity in runoff dynamics is likely to result in differential responses to disturbances, influencing catchment-scale hydrologic resilience and recovery. In the wet forests of the Pacific Northwest, where the Lookout Creek catchment is located, future climate scenarios depict increasing wildfire activity (Dye et al. 2024; Halofsky et al. 2020; Holden et al. 2018). Wildfire in this region can have catastrophic

impacts on forest values and services because these ecosystems are the main source of water for downstream communities and ecosystems (Wampler et al. 2023). The role of storage on the heterogeneity of streamflow generation that we observed is important for developing mechanistic understandings of how the water cycle will change following wildfire. We expect that hydrologic resilience will be mediated by storage. As such, this study can inform management strategies of montane water resources. For example, work emerging from lower elevation watersheds within Lookout Creek following the low to moderately severe 2021 Holiday Farm Fire suggested changes in flow paths and baseflow, 2 years post fire in watersheds with relatively low storage (Bush et al. 2024). The work here offers an unprecedented opportunity to understand how differences in storage play a role in mitigating the impacts of fire on water and nutrient cycling, as many of the catchments studied here were burned in late 2023 following the conclusion of this study.

5 | Conclusions

Our study illustrates how variability in storage across catchments gives rise to heterogeneous streamflow generation mechanisms in small mountainous catchments and their importance for flow in a larger 5th-order stream. We found strong variability in hydrologic regimes (based on hydrometric records), variable spatial and seasonal dynamics of water stable isotopes that, combined with precipitation information, highlight the importance of fall and winter storms to year-round streamflow and the strong control that earthflows and landslide deposits have on storage variability. Our analysis included 10 years of weekly precipitation and 1 year of weekly stream samples in 10 locations analysed for water isotope ratios. We showed wide variability in storage and water contributions from perennial tributaries to the main stem of Lookout Creek. In many cases, the relative water contributions from each tributary varied seasonally. This analysis highlights the overwhelming importance of some tributaries to the maintenance of summer flows. Most notably, the contributions of Cold and Longer Creeks, which are <4 km^2, sustain up to 50% of the streamflow in the 64 km^2 Lookout Creek catchment during the summer months. Streamflow in Cold and Longer Creeks varied very little as compared to other streams in which streamflow varied seasonally. The variation in headwater streams within the 5th-order 64 km^2 catchment illustrates how geomorphic complexity can influence the distribution of streamflow and the sensitivity of larger streams to dry and wet periods.

Acknowledgements

Jaime Ortega acknowledges the support of SENACYT (Secretaría Nacional de Ciencia, Tecnología e Innovación) of Panamá for providing a scholarship. Catalina Segura acknowledges the National Science Foundation (NSF) Award No. EAR-1943574. Catalina Segura and Pamela L. Sullivan acknowledge the NSF Award No. EAR-2424997. Pamela L. Sullivan acknowledges the NSF Awards No. EAR-2034232 and EAR-2012796. We would like to thank all members of the Segura and Sullivan research groups for insightful discussions, Mark Schulze, Greg Dowing, and Greg Cohn for assistance collecting precipitation samples, and Julia Jones and Daniele Penna for helpful discussions. Streamflow and climate data were provided by the H.J. Andrews Experimental Forest and Long-Term Ecological Research (LTER) program, administered cooperatively by Oregon State University, the USDA Forest Service Pacific Northwest Research Station, and the Willamette National Forest. This material is based upon work supported by the National Science Foundation under the grant LTER8 DEB-2025755. This manuscript has been subjected to Agency review and has been approved for publication. The views expressed in this paper are those of the author(s) and do not necessarily reflect the views or policies of the U.S. Environmental Protection Agency. Mention of trade names or commercial products does not constitute endorsement or recommendation for use.

Data Availability Statement

The data that support the findings of this study are openly available in HJ Andrews Experimental Forest LTER at https://andrewsforest.oregonstate.edu/, reference number MS001, HF028, HF004, GE009, GE010, GI010. https://doi.org/10.6073/pasta/f7bfbab3132ac23002d5df6e837a9d.

References

Alexander, R. B., E. W. Boyer, R. A. Smith, G. E. Schwarz, and R. B. Moore. 2007. "The Role of Headwater Streams in Downstream Water Quality1." *JAWRA Journal of the American Water Resources Association* 43, no. 1: 41–59.

Araguas-Araguas, L., K. Froehlich, and K. Rozanski. 2000. "Deuterium and Oxygen-18 Isotope Composition of Precipitation and Atmospheric Moisture." *Hydrological Processes* 14, no. 8: 1341–1355.

Asano, Y., M. Kawasaki, T. Saito, et al. 2020. "An Increase in Specific Discharge With Catchment Area Implies That Bedrock Infiltration Feeds Large Rather Than Small Mountain Headwater Streams." *Water Resources Research* 56, no. 9: 25658.

Bansah, S., and G. Ali. 2019. "Streamwater Ages in Nested, Seasonally Cold Canadian Watersheds." *Hydrological Processes* 33, no. 4: 495–511.

Barnhart, T. B., C. L. Tague, and N. P. Molotch. 2020. "The Counteracting Effects of Snowmelt Rate and Timing on Runoff." *Water Resources Research* 56, no. 8. https://doi.org/10.1029/2019wr026634.

Befus, K. M., A. F. Sheehan, M. Leopold, S. P. Anderson, and R. S. Anderson. 2011. "Seismic Constraints on Critical Zone Architecture, Boulder Creek Watershed, Front Range, Colorado." *Vadose Zone Journal* 10, no. 3: 915–927.

Benettin, P., N. B. Rodriguez, M. Sprenger, et al. 2022. "Transit Time Estimation in Catchments: Recent Developments and Future Directions." *Water Resources Research* 58, no. 11: 33096.

Benjamin, L., L. L. Knobel, L. F. Hall, L. D. Cecil, and J. R. Green. 2005. Development of a Local Meteoric Water Line for Southeastern Idaho, Western Wyoming, and South-Central Montana.

Berghuijs, W. R., R. A. Woods, and M. Hrachowitz. 2014. "A Precipitation Shift From Snow Towards Rain Leads to a Decrease in Streamflow." *Nature Climate Change* 4, no. 7: 583–586.

Beria, H., J. R. Larsen, N. C. Ceperley, A. Michelon, T. Vennemann, and B. Schaefli. 2018. "Understanding Snow Hydrological Processes Through the Lens of Stable Water Isotopes." *WIREs Water* 5, no. 6: e1311.

Bershaw, J., S. M. Penny, and C. N. Garzione. 2012. "Stable Isotopes of Modern Water Across the Himalaya and Eastern Tibetan Plateau: Implications for Estimates of Paleoelevation and Paleoclimate." *Journal of Geophysical Research: Atmospheres*: D02110. https://doi.org/10.1029/2011JD016132.

Bershaw, J., J. E. Saylor, C. N. Garzione, A. Leier, and K. E. Sundell. 2016. "Stable Isotope Variations (Delta O-18 and Delta D) in Modern Waters Across the Andean Plateau." *Geochimica et Cosmochimica Acta* 194: 310–324.

Bierlmaier, F. A., and A. McKee. 1989. "Climatic Summaries and Documentation for the Primary Meteorological Station, H.J. Andrews

Experimental Forest, 1972 to 1984." Technical Report PNW-GTR-242: 61. https://doi.org/10.2737/PNW-GTR-242.

Birkel, C., A. Correa-Barahona, M. Martinez-Martinez, et al. 2020. "Headwaters Drive Streamflow and Lowland Tracer Export in a Large-Scale Humid Tropical Catchment." *Hydrological Processes* 34, no. 18: 3824–3841.

Birkel, C., C. Soulsby, and D. Tetzlaff. 2011. "Modelling Catchment-Scale Water Storage Dynamics: Reconciling Dynamic Storage With Tracer-Inferred Passive Storage." *Hydrological Processes* 25: 3924–3936.

Bowen, G. J., Z. Cai, R. P. Fiorella, and A. L. Putman. 2019. "Isotopes in the Water Cycle: Regional-To Global-Scale Patterns and Applications." *Annual Review of Earth and Planetary Sciences* 47, no. 1: 453–479.

Bowen, G. J., and J. Revenaugh. 2003. "Interpolating the Isotopic Composition of Modern Meteoric Precipitation." *Water Resources Research* 39, no. 10: 1299. https://doi.org/10.1029/2003WR002086.

Bowen, G. J., and B. Wilkinson. 2002. "Spatial Distribution of δ18O in Meteoric Precipitation." *Geology* 30, no. 4: 315–318.

Brantley, S. L., W. H. McDowell, W. E. Dietrich, et al. 2017. "Designing a Network of Critical Zone Observatories to Explore the Living Skin of the Terrestrial Earth." *Earth Surface Dynamics* 5, no. 4: 841–860.

Brooks, J. R. 2025. *Water Stable Isotope Data from the Willamette Basin, Oregon*. U.S. EPA Office of Research and Development (ORD). https://doi.org/10.23719/1531963.

Brooks, J. R., W. D. Rugh, and R. A. Werner. 2022. "Tree-Ring Stable Isotope Measurements: The Role of Quality Assurance and Quality Control to Ensure High Quality Data." In *Stable Isotopes in Tree Rings: Inferring Physiological, Climatic and Environmental Responses*, edited by R. T. W. Siegwolf, J. R. Brooks, J. Roden, and M. Saurer, 191–213. Springer International Publishing.

Brooks, J. R., P. J. Wigington, D. L. Phillips, R. Comeleo, and R. Coulombe. 2012. "Willamette River Basin Surface Water Isoscape (Delta O-18 and Delta H-2): Temporal Changes of Source Water Within the River." *Ecosphere* 3, no. 5: 21.

Bush, S. A., S. L. Johnson, K. D. Bladon, and P. L. Sullivan. 2024. "Stream Chemical Response Is Mediated by Hydrologic Connectivity and Fire Severity in a Pacific Northwest Forest." *Hydrological Processes* 38, no. 7: e15231.

Buttle, J. M. 2018. "Mediating Stream Baseflow Response to Climate Change: The Role of Basin Storage." *Hydrological Processes* 32, no. 3: 363–378.

Calvi, C., E. Carol, L. Fennell, and M. Naipauer. 2024. "Assessment of Hydrological Systems Associated With Groundwater Discharges in Arid High Mountain Environments of the Argentine Andes." *Groundwater for Sustainable Development* 26: 101218.

Ciais, P., and J. Jouzel. 1994. "Deuterium and Oxygen-18 in Precipitation—Isotopic Model, Including Mixed Cloud Processes." *Journal of Geophysical Research-Atmospheres* 99, no. D8: 16793–16803.

Clark, I. D., and P. Fritz. 1997. *Environmental Isotopes in Hydrogeology*. Taylor & Francis.

Craig, H. 1961. "Isotopic Variations in Meteoric Waters." *Science* 133, no. 3465: 1702–1703.

Crampe, E. A., C. Segura, and J. A. Jones. 2021. "Fifty Years of Runoff Response to Conversion of Old-Growth Forest to Planted Forest in the H. J. Andrews Forest, Oregon, USA." *Hydrological Processes* 35, no. 5: e14168.

Daly, C., M. Schulze, and W. McKee. 2025. "Meteorological Data From Benchmark Stations at the HJ Andrews Experimental Forest, 1957 to Present." In *Long-Term Ecological Research*. Forest Science Data Bank. http://andlter.forestry.oregonstate.edu/data/abstract.aspx?dbcode=MS001.

Dierauer, J. R., P. H. Whitfield, and D. M. Allen. 2018. "Climate Controls on Runoff and Low Flows in Mountain Catchments of Western North America." *Water Resources Research* 54, no. 10: 7495–7510.

Dingman, S. L. 2002. *Physical Hydrology*. Prentice Hall.

Dogramaci, S., G. Skrzypek, W. Dodson, and P. F. Grierson. 2012. "Stable Isotope and Hydrochemical Evolution of Groundwater in the Semi-Arid Hamersley Basin of Subtropical Northwest Australia." *Journal of Hydrology* 475: 281–293.

Dye, A. W., M. J. Reilly, A. McEvoy, et al. 2024. "Simulated Future Shifts in Wildfire Regimes in Moist Forests of Pacific Northwest, USA." *Journal of Geophysical Research: Biogeosciences* 129, no. 2: e2023JG007722.

England, J. F., T. A. Cohn, B. A. Faber, et al. 2018. "Guidelines for Determining Flood Flow Frequency—Bulletin 17C." *Techniques and Methods 4-B5*: 168.

Fan, Y., L. Toran, and R. W. Schlische. 2007. "Groundwater Flow and Groundwater-Stream Interaction in Fractured and Dipping Sedimentary Rocks: Insights From Numerical Models." *Water Resources Research* 43: W01409. https://doi.org/10.1029/2006WR004864.

Fennell, J., J. Geris, M. E. Wilkinson, R. Daalmans, and C. Soulsby. 2020. "Lessons From the 2018 Drought for Management of Local Water Supplies in Upland Areas: A Tracer-Based Assessment." *Hydrological Processes* 34, no. 22: 4190–4210.

Floriancic, M. G., B. M. C. Fischer, P. Molnar, J. W. Kirchner, and I. H. J. van Meerveld. 2019. "Spatial Variability in Specific Discharge and Streamwater Chemistry During Low Flows: Results From Snapshot Sampling Campaigns in Eleven Swiss Catchments." *Hydrological Processes* 33, no. 22: 2847–2866.

Freeman, M. C., C. M. Pringle, and C. R. Jackson. 2007. "Hydrologic Connectivity and the Contribution of Stream Headwaters to Ecological Integrity at Regional Scales1." *JAWRA Journal of the American Water Resources Association* 43, no. 1: 5–14.

Gat, J. R. 2010. *Isotope Hydrology: A Study of the Water Cycle*. Imperial College Press.

Gat, J. R., and E. Matsui. 1991. "Atmospheric Water-Balance in the Amazon Basin—An Isotopic Evapotranspiration Model." *Journal of Geophysical Research-Atmospheres* 96, no. D7: 13179–13188.

Genereux, D. 1998. "Quantifying Uncertainty in Tracer-Based Hydrograph Separations." *Water Resources Research* 34: 915–919.

Gomi, T., R. C. Sidle, and J. S. Richardson. 2002. "Understanding Processes and Downstream Linkages of Headwater Systems." *Bioscience* 52: 905–916.

Gonfiantini, R., M.-A. Roche, J.-C. Olivry, J.-C. Fontes, and G. M. Zuppi. 2001. "The Altitude Effect on the Isotopic Composition of Tropical Rains." *Chemical Geology* 181, no. 1: 147–167.

Goodman, A. C., C. Segura, J. A. Jones, and F. J. Swanson. 2023. "Seventy Years of Watershed Response to Floods and Changing Forestry Practices in Western Oregon, USA." *Earth Surface Processes and Landforms* 48: esp.5537.

Groning, M., H. O. Lutz, Z. Roller-Lutz, M. Kralik, L. Gourcy, and L. Poltenstein. 2012. "A Simple Rain Collector Preventing Water Re-Evaporation Dedicated for Delta O-18 and Delta H-2 Analysis of Cumulative Precipitation Samples." *Journal of Hydrology* 448: 195–200.

Hale, K. E., K. N. Musselman, A. J. Newman, B. Livneh, and N. P. Molotch. 2023. "Effects of Snow Water Storage on Hydrologic Partitioning Across the Mountainous, Western United States." *Water Resources Research* 59, no. 8: e2023WR034690.

Halofsky, J. E., D. L. Peterson, and B. J. Harvey. 2020. "Changing Wildfire, Changing Forests: The Effects of Climate Change on Fire Regimes and Vegetation in the Pacific Northwest, USA." *Fire Ecology* 16, no. 1: 4.

Herschy, R. W. 2009. *Streamflow Measurement*. CRC Press.

Holden, Z. A., A. Swanson, C. H. Luce, et al. 2018. "Decreasing Fire Season Precipitation Increased Recent Western US Forest Wildfire Activity." *Proceedings of the National Academy of Sciences of the United States of America* 115, no. 36: E8349–E8357.

Huang, C.-C., and H.-F. Yeh. 2022. "Evaluation of Seasonal Catchment Dynamic Storage Components Using an Analytical Streamflow Duration Curve Model." *Sustainable Environment Research* 32, no. 1: 49.

Hughes, C. E., and J. Crawford. 2012. "A New Precipitation Weighted Method for Determining the Meteoric Water Line for Hydrological Applications Demonstrated Using Australian and Global GNIP Data." *Journal of Hydrology* 464: 344–351.

Jasechko, S. 2019. "Global Isotope Hydrogeology—Review." *Reviews of Geophysics* 57, no. 3: 835–965.

Jeelani, G., U. Saravana Kumar, and B. Kumar. 2013. "Variation of δ18O and δD in Precipitation and Stream Waters Across the Kashmir Himalaya (India) to Distinguish and Estimate the Seasonal Sources of Stream Flow." *Journal of Hydrology* 481: 157–165.

Jefferson, A., G. Grant, and T. Rose. 2006. "Influence of Volcanic History on Groundwater Patterns on the West Slope of the Oregon High Cascades." *Water Resources Research* 42: W12411. https://doi.org/10.1029/2005WR004812.

Jennings, K., and J. A. Jones. 2015. "Precipitation-Snowmelt Timing and Snowmelt Augmentation of Large Peak Flow Events, Western Cascades, Oregon." *Water Resources Research* 51, no. 9: 7649–7661.

Jódar, J., J. A. Cabrera, S. Martos-Rosillo, et al. 2017. "Groundwater Discharge in High-Mountain Watersheds: A Valuable Resource for Downstream Semi-Arid Zones. The Case of the Bérchules River in Sierra Nevada (Southern Spain)." *Science of the Total Environment* 593: 760–772.

Johnson, K., J. N. Christensen, W. P. Gardner, et al. 2024. "Shifting Groundwater Fluxes in Bedrock Fractures: Evidence From Stream Water Radon and Water Isotopes." *Journal of Hydrology* 635: 131202.

Johnson, K., A. Harpold, R. W. H. Carroll, et al. 2023. "Leveraging Groundwater Dynamics to Improve Predictions of Summer Low-Flow Discharges." *Water Resources Research* 59, no. 8: e2023WR035126.

Johnson, K., K. H. Williams, J. N. Christensen, et al. 2025. "Hidden Features: How Subsurface and Landscape Heterogeneity Govern Hydrologic Connectivity and Stream Chemistry in a Montane Watershed." *Hydrological Processes* 39, no. 3: e70085.

Johnson, S. L., S. M. Wondzell, J. S. Rothacher, and J. A. Jones. 2024. *Stream Discharge in Gaged Watersheds at the HJ Andrews Experimental Forest, 1949 to Present. Long-Term Ecological Research*. Forest Science Data Bank. http://andlter.forestry.oregonstate.edu/data/abstract.aspx?dbcode=HF004.

Jones, J. A., and R. M. Perkins. 2010. "Extreme Flood Sensitivity to Snow and Forest Harvest, Western Cascades, Oregon, United States." *Water Resources Research* 46, no. 12: 2009WR008632.

Jung, Y. Y., D. C. Koh, W. J. Shin, H. I. Kwon, Y. H. Oh, and K. S. Lee. 2021. "Assessing Seasonal Variations in Water Sources of Streamflow in a Temperate Mesoscale Catchment With Granitic Bedrocks Using Hydrochemistry and Stable Isotopes." *Journal of Hydrology: Regional Studies* 38: 100940.

Karlstrom, L., N. Klema, G. E. Grant, et al. 2025. "State Shifts in the Deep Critical Zone Drive Landscape Evolution in Volcanic Terrains." *Proceedings of the National Academy of Sciences of the United States of America* 122, no. 3: e2415155122.

Kendall, C., and T. B. Coplen. 2001. "Distribution of Oxygen-18 and Deuterium in River Waters Across the United States." *Hydrological Processes* 15, no. 7: 1363–1393.

Kirchner, J. W., D. Tetzlaff, and C. Soulsby. 2010. "Comparing Chloride and Water Isotopes as Hydrological Tracers in Two Scottish Catchments." *Hydrological Processes* 24, no. 12: 1631–1645.

Knowles, N., M. D. Dettinger, and D. R. Cayan. 2006. "Trends in Snowfall Versus Rainfall in the Western United States." *Journal of Climate* 19, no. 18: 4545–4559.

Kruskal, W. H., and W. A. Wallis. 1952. "Use of Ranks in One-Criterion Variance Analysis." *Journal of the American Statistical Association* 47, no. 260: 583–621.

Lane, C. R., I. F. Creed, H. E. Golden, et al. 2023. "Vulnerable Waters Are Essential to Watershed Resilience." *Ecosystems* 26, no. 1: 1–28.

Leibowitz, S. G., D. M. Mushet, and W. E. Newton. 2016. "Intermittent Surface Water Connectivity: Fill and Spill vs. Fill and Merge Dynamics." *Wetlands* 36, no. s2: 323–342.

Leuthold, S. J., S. A. Ewing, R. A. Payn, F. R. Miller, and S. G. Custer. 2021. "Seasonal Connections Between Meteoric Water and Streamflow Generation Along a Mountain Headwater Stream." *Hydrological Processes* 35: e14029. https://doi.org/10.1002/hyp.14029.

Li, D. Y., M. L. Wrzesien, M. Durand, J. Adam, and D. P. Lettenmaier. 2017. "How Much Runoff Originates as Snow in the Western United States, and How Will That Change in the Future?" *Geophysical Research Letters* 44, no. 12: 6163–6172.

Liotta, M., F. Grassa, W. D'Alessandro, et al. 2013. "Isotopic Composition of Precipitation and Groundwater in Sicily, Italy." *Applied Geochemistry* 34: 199–206.

Litwin, D. G., G. E. Tucker, K. R. Barnhart, and C. J. Harman. 2022. "Groundwater Affects the Geomorphic and Hydrologic Properties of Coevolved Landscapes." *Journal of Geophysical Research Earth Surface* 127: e2021JF006239. https://doi.org/10.1029/2021JF006239.

Lyon, S. W., M. Nathanson, A. Spans, et al. 2012. "Specific Discharge Variability in a Boreal Landscape." *Water Resources Research* 48: W08506. https://doi.org/10.1029/2011WR011073.

Maloszewski, P., W. Rauert, W. Stichler, and A. Herrmann. 1983. "Application of Flow Models in an Alpine Catchment-Area Using Tritium and Deuterium Data." *Journal of Hydrology* 66, no. 1–4: 319–330.

Martinelli, L. A., R. L. Victoria, L. Silveira Lobo Sternberg, A. Ribeiro, and M. Zacharias Moreira. 1996. "Using Stable Isotopes to Determine Sources of Evaporated Water to the Atmosphere in the Amazon Basin." *Journal of Hydrology* 183, no. 3: 191–204.

McGill, L. M., J. R. Brooks, and E. A. Steel. 2021. "Spatiotemporal Dynamics of Water Sources in a Mountain River Basin Inferred Through δ2H and δ18O of Water." *Hydrological Processes* 35, no. 3: e14063.

McGlynn, B. L., J. J. McDonnel, and D. D. Brammer. 2002. "A Review of the Evolving Perceptual Model of Hillslope Flowpaths at the Maimai Catchments, New Zealand." *Journal of Hydrology* 257, no. 1–4: 1–26.

McGuire, K. J., and J. J. McDonnell. 2006. "A Review and Evaluation of Catchment Transit Time Modeling." *Journal of Hydrology* 330: 543–563.

McGuire, K. J., J. J. McDonnell, M. Weiler, et al. 2005. "The Role of Topography on Catchment-Scale Water Residence Time." *Water Resources Research* 41, no. 5: W05002.

McMillan, H., I. Westerberg, and F. Branger. 2017. "Five Guidelines for Selecting Hydrological Signatures." *Hydrological Processes* 31: 4757–4761.

Meyer, J. L., D. L. Strayer, J. B. Wallace, S. L. Eggert, G. S. Helfman, and N. E. Leonard. 2007. "The Contribution of Headwater Streams to Biodiversity in River Networks1." *JAWRA Journal of the American Water Resources Association* 43, no. 1: 86–103.

Moore, D. R., and S. Wondzell. 2005. "Physical Hydrology and the Effects of Forest Harvesting in the Pacific Northwest: A Review." *Journal of the American Water Resources Association* 41, no. 4: 763–784.

Mote, P. W., S. Li, D. P. Lettenmaier, M. Xiao, and R. Engel. 2018. "Dramatic Declines in Snowpack in the Western US." *npj Climate and Atmospheric Science* 1, no. 1: 2.

Müller, S., C. Stumpp, J. H. Sorensen, and S. Jessen. 2017. "Spatiotemporal Variation of Stable Isotopic Composition in Precipitation: Post-Condensational Effects in a Humid Area." *Hydrological Processes* 31, no. 18: 3146–3159.

Nickolas, L. B., C. Segura, and J. R. Brooks. 2017. "The Influence of Lithology on Surface Water Sources." *Hydrological Processes* 31, no. 10: 1913–1925.

Ortega, J. 2024. *Driver of Relative Streamflow Contribution in Mountainous Headwater Streams*. Masters Thesis.

Peng, T.-R., K.-Y. Chen, W.-J. Zhan, W.-C. Lu, and L.-T. J. Tong. 2015. "Use of Stable Water Isotopes to Identify Hydrological Processes of Meteoric Water in Montane Catchments." *Hydrological Processes* 29, no. 23: 4957–4967.

Perry, T. D., and J. A. Jones. 2017. "Summer Streamflow Deficits From Regenerating Douglas-Fir Forest in the Pacific Northwest, USA." *Ecohydrology* 10, no. 2: e1790.

Phillips, D. L., and J. W. Gregg. 2003. "Source Partitioning Using Stable Isotopes: Coping With Too Many Sources." *Oecologia* 136, no. 2: 261–269.

Phillips, D. L., S. D. Newsome, and J. W. Gregg. 2005. "Combining Sources in Stable Isotope Mixing Models: Alternative Methods." *Oecologia* 144, no. 4: 520–527.

Poage, M. A., and C. P. Chamberlain. 2001. "Empirical Relationships Between Elevation and the Stable Isotope Composition of Precipitation and Surface Waters: Considerations for Studies of Paleoelevation Change." *American Journal of Science* 301, no. 1: 1–15.

Putman, A. L., R. P. Fiorella, G. J. Bowen, and Z. Cai. 2019. "A Global Perspective on Local Meteoric Water Lines: Meta-Analytic Insight Into Fundamental Controls and Practical Constraints." *Water Resources Research* 55, no. 8: 6896–6910.

Qu, D., L. Tian, H. Zhao, P. Yao, B. Xu, and J. Cui. 2020. "Demonstration of a Memory Calibration Method in Water Isotope Measurement by Laser Spectroscopy." *Rapid Communications in Mass Spectrometry* 34, no. 8: e8689.

Safeeq, M., and C. T. Hunsaker. 2016. "Characterizing Runoff and Water Yield for Headwater Catchments in the Southern Sierra Nevada." *JAWRA Journal of the American Water Resources Association* 52, no. 6: 1327–1346.

Sánchez-Murillo, R., E. S. Brooks, W. J. Elliot, and J. Boll. 2015. "Isotope Hydrology and Baseflow Geochemistry in Natural and Human-Altered Watersheds in the Inland Pacific Northwest, USA." *Isotopes in Environmental and Health Studies* 51, no. 2: 231–254.

Sawicz, K., T. Wagener, M. Sivapalan, P. A. Troch, and G. Carrillo. 2011. "Catchment Classification: Empirical Analysis of Hydrologic Similarity Based on Catchment Function in the Eastern USA." *Hydrology and Earth System Sciences* 15, no. 9: 2895–2911.

Seabold, S., and J. Perktold. 2010. *Statsmodels: Econometric and Statistical Modeling With Python*. 9th Python in Science Conference, Austin, 28 June-3 July, 2010, 57–61.

Segura, C. 2021. "Snow Drought Reduces Water Transit Times in Headwater Streams." *Hydrological Processes* 35, no. 12: e14437.

Segura, C., D. Noone, D. Warren, J. A. Jones, J. Tenny, and L. Ganio. 2019. "Climate, Landforms, and Geology Affect Baseflow Sources in a Mountain Catchment." *Water Resources Research* 55: 5238–5254.

Segura, C., Z. Perry, and J. Ortega. 2024. "Water Stable Isotopes for Streams and Precipitation Samples in the HJ Andrews Experimental Forest, 2014–2023." In *Long-Term Ecological Research*. Forest Science Data Bank. http://andlter.forestry.oregonstate.edu/data/abstract.aspx?dbcode=HF028.

Siirila-Woodburn, E. R., A. M. Rhoades, B. J. Hatchett, et al. 2021. "A Low-To-No Snow Future and Its Impacts on Water Resources in the Western United States." *Nature Reviews Earth and Environment* 2, no. 11: 800–819.

Sklash, M. G., and R. N. Farvolden. 1979. "Role of Groundwater in Storm Runoff." *Journal of Hydrology* 43: 45–65.

Somers, L. D., and J. M. McKenzie. 2020. "A Review of Groundwater in High Mountain Environments." *WIREs Water* 7, no. 6: e1475.

Soulsby, C., C. Birkel, J. Geris, and D. Tetzlaff. 2015. "Spatial Aggregation of Time-Variant Stream Water Ages in Urbanizing Catchments." *Hydrological Processes* 29, no. 13: 3038–3050.

Soulsby, C., R. Malcolm, R. Helliwell, R. C. Ferrier, and A. Jenkins. 2000. "Isotope Hydrology of the Allt a' Mharcaidh Catchment, Cairngorms, Scotland: Implications for Hydrological Pathways and Residence Times." *Hydrological Processes* 14, no. 4: 747–762.

Soulsby, C., K. Piegat, J. Seibert, and D. Tetzlaff. 2011. "Catchment-Scale Estimates of Flow Path Partitioning and Water Storage Based on Transit Time and Runoff Modelling." *Hydrological Processes* 25: 3960–3976.

Soulsby, C., D. Tetzlaff, P. Rodgers, S. Dunn, and S. Waldron. 2006. "Runoff Processes, Stream Water Residence Times and Controlling Landscape Characteristics in a Mesoscale Catchment: An Initial Evaluation." *Journal of Hydrology* 325: 197–221.

Spence, C. 2007. "On the Relation Between Dynamic Storage and Runoff: A Discussion on Thresholds, Efficiency, and Function." *Water Resources Research* 43: W12416. https://doi.org/10.1029/2006WR005645.

Spies, T. A. 2013. "LiDAR Data (August 2008) for the Andrews Experimental Forest and Willamette National Forest Study Areas [Data Set]." *Environmental Data Initiative*. https://doi.org/10.6073/PASTA/C47128D6C63DFF39EE48604ECC6FABFC.

Sprenger, M., R. W. H. Carroll, D. Marchetti, et al. 2024. "Stream Water Sourcing From High-Elevation Snowpack Inferred From Stable Isotopes of Water: A Novel Application of d-Excess Values." *Hydrology and Earth System Sciences* 28, no. 7: 1711–1723.

St Clair, J., S. Moon, W. S. Holbrook, et al. 2015. "Geophysical Imaging Reveals Topographic Stress Control of Bedrock Weathering." *Science* 350, no. 6260: 534–538.

Staudinger, M., M. Stoelzle, S. Seeger, J. Seibert, M. Weiler, and K. Stahl. 2017. "Catchment Water Storage Variation With Elevation." *Hydrological Processes* 31, no. 11: 2000–2015. https://doi.org/10.1002/hyp.11158.

Stock, B. C., A. L. Jackson, E. J. Ward, A. C. Parnell, D. L. Phillips, and B. X. Semmens. 2018. "Analyzing Mixing Systems Using a New Generation of Bayesian Tracer Mixing Models." *PeerJ* 6: e5096.

Swanson, F. J. 2005. "Upper Blue River Geology Clipped to the Andrews Experimental Forest, 1991." In *Long-Term Ecological Research*. Forest Science Data Bank. http://andlter.forestry.oregonstate.edu/data/abstract.aspx?dbcode=GE009.

Swanson, F. J. 2013. "Mass Movement Assessment: Cascade Hazards Ratings, Andrews Experimental Forest, 1992." In *Long-Term Ecological Research*. Forest Science Data Bank. http://andlter.forestry.oregonstate.edu/data/abstract.aspx?dbcode=GE010.

Swanson, F., and M. James. 1975. "Geology and Geomorphology of the H.J. Andrews Experimental Forest, Western Cascades, Oregon." Research Paper PNW-188. Portland, OR: U.S. Department of Agriculture, Forest Service, Pacific Northwest Forest and Range Experiment Station, 14.

Thurber, D., B. Lane, T. F. Xu, and B. T. Neilson. 2024. "Dissolving the Mystery of Subsurface Controls on Snowmelt-Discharge Dynamics in Karst Mountain Watersheds Using Hydrologic Timeseries." *Hydrological Processes* 38, no. 5: e15170.

Uhlenbrook, S., M. Frey, C. Leibundgut, and P. Maloszewski. 2002. "Hydrograph Separations in a Mesoscale Mountainous Basin at Event

and Seasonal Timescales." *Water Resources Research* 38, no. 6. https://doi.org/10.1029/2001WR000938.

Vano, J. A., B. Nijssen, and D. P. Lettenmaier. 2015. "Seasonal Hydrologic Responses to Climate Change in the Pacific Northwest." *Water Resources Research* 51, no. 4: 1959–1976.

Verfaillie, D., M. Lafaysse, M. Déqué, N. Eckert, Y. Lejeune, and S. Morin. 2018. "Multi-Component Ensembles of Future Meteorological and Natural Snow Conditions for 1500 m Altitude in the Chartreuse Mountain Range, Northern French Alps." *Cryosphere* 12, no. 4: 1249–1271.

Voss, K. A., B. Bookhagen, D. Sachse, and O. A. Chadwick. 2020. "Variation of Deuterium Excess in Surface Waters Across a 5000-m Elevation Gradient in Eastern Nepal." *Journal of Hydrology* 586: 124802.

Wampler, K. A., K. D. Bladon, and M. Faramarzi. 2023. "Modeling Wildfire Effects on Streamflow in the Cascade Mountains, Oregon, USA." *Journal of Hydrology* 621: 129585.

Wassenaar, L. I., P. Athanasopoulos, and M. J. Hendry. 2011. "Isotope Hydrology of Precipitation, Surface and Ground Waters in the Okanagan Valley, British Columbia, Canada." *Journal of Hydrology* 411, no. 1–2: 37–48.

Weiler, M., J. J. McDonnell, I. Tromp-van Meerveld, and T. Uchida. 2006. "Subsurface Stormflow." In *Encyclopedia of Hydrological Sciences*, edited by M. G. Anderson, and J. J. McDonnell. https://doi.org/10.1002/0470848944.hsa119.

Windler, G., J. R. Brooks, H. M. Johnson, R. L. Comeleo, R. Coulombe, and G. J. Bowen. 2021. "Climate Impacts on Source Contributions and Evaporation to Flow in the Snake River Basin Using Surface Water Isoscapes (δ2H and δ18O)." *Water Resources Research* 57, no. 7: e2020WR029157.

Yao, L. L., A. Sankarasubramanian, and D. B. Wang. 2021. "Climatic and Landscape Controls on Long-Term Baseflow." *Water Resources Research* 57, no. 6: e2020WR029284.

Supporting Information

Additional supporting information can be found online in the Supporting Information section. **Figure S1:** Monthly average precipitation and streamflow at the meteorological station PRIMET and Lookout Creek at the USGS station (No. 14161500). The figure includes long-term records and study period (May 2022–May 2023). The error bars are the monthly standard deviation. **Figure S2:** Overlapping samples ($n = 164$) collected in Corvallis and PRIMET between 2014 and 2023; (B) Dual isotope line for the overlapping isotope ratios in A; (C) relationship between precipitation amount and the ratio of isotope rations in Corvallis and isotope ratios in PRIMET. The dash line indicated a 10 mm threshold over which we can build a robust relationship. **Figure S3:** Relationship between isotope ratios in Corvallis and isotope ratios in PRIMET. We included samples that correspond to > 10 mm of rain in Corvallis. These relationships were used to estimate isotope ratios in Corvallis when access to the H.J. Experimental Forest was not possible during the 2019–2020 fire season. **Table S1:** General hydrological information of the gauged catchments of Cold, Longer, Mack, and Lookout Creeks. **Table S2:** Daily streamflow characteristics by gauged catchments derived from the flow duration curve analysis (FDC). **Table S3:** Volume weighted average and standard deviation (σ) of precipitation isotopic ratios ($\overline{\overline{\delta^{18}O}}$, $\overline{\overline{\delta^{2}H}}$, and $\overline{\overline{d}}$) at PRIMET. **Table S4:** Volume-weighted average and standard deviation (σ) in seasonal precipitation isotopic values (2015–2023) at PRIMET. Values with different letters are significantly different from each other ($p < 0.05$), ANOVA- Tukey test. **Table S5:** Summary of regression coefficients (a: slope and b: intercept and standard errors, σ) and R^2 for seasonal and 2015–2023 volume-weighted Local Meteoric Water lines (LMWL) at PRIMET. The number of samples (n) used in each LMWL is also indicated. Slopes or intercepts with different letters are significantly different from each other (ANCOVA, $p < 0.05$). The * indicates significant differences with the GMWL slope of 8 or intercept of 10. **Figure S4:** Precipitation isotopic signature $\delta^{18}O$ (A) and d-excess (B) throughout time (water years: 2015–2023). Black line represents the volume weighted moving average with a window of 25 values. Seasons were defined as: spring (03/20–06/20), summer (06/21–09/22), fall (09/23–12/20), and winter (12/21–03/19). **Table S6:** Summary of the isotope ratios ($\delta^{18}O$, $\delta^{2}H$) and deuterium excess ($\overline{d}$-excess) from stream samples across seasons and stream classification. **Table S7:** χ^2 and p values of the seasonal† differences (Kruskal-Wallis test) in median and median standard deviations of $\delta^{18}O$ and $\delta^{2}H$, and d-excess in stream samples (Table S6). Values are in bold if $p < 0.05$. **Table S8:** Seasonal† and study period isotopic lapse rates based on averages isotopic values ($\overline{\delta^{18}O}$, $\overline{\delta^{2}H}$, and $\overline{d}$-excess) for stream samples. Lapse rates are described in terms of regression coefficients: slope (a) and intercept (b), with associated standard deviations (σ), coefficient of determination (R^2) and corresponding p value of the relationship. **Figure S5:** Damping ratio relationship ($\delta^{18}O$ vs. $\delta^{2}H$) by analysed catchment for the study period. Ratios were compared relative to the 1:1 line (dashed black diagonal line). A are values derived considering all samples and B are values derived, omitting one sample per site collected during the Nov 5, 2022, storm event. Tributaries (triangles) are Cold (CC), Longer (LC), Mack (MC), Nostoc (NC), McRae (MR) Creeks. Mainstem location in Lookout Creek (circles) are LO1–LO5 are shown in Figure 1. **Figure S6:** Seasonal average d-excess across sampling sites during the study period. Shaded areas depict the seasonal volume-weighted average precipitation d-excess. Tributaries (triangles) are Cold (CC), Longer (LC), Mack (MC), Nostoc (NC), McRae (MR) Creeks. Mainstem location in Lookout Creek (circles) are LO1–LO5 (Figure 1). **Table S9:** Hydrograph separation in the event and pre-event water for a fall precipitation event between 01-Nov-2022-and 06-Nov-2022 at the 10 sampling sites. CC is Cold Creek, LC is Longer Creek, MC is Mack Creek, NC, Nostoc Creek, MR is McRae Creek and LO1–LO5 are sites in the main stem of Lookout Creek (Figure 1). Two pre-event estimates (Pre-event$_1$ and Pre-sevnt$_2$) were based on 2 different possible input concentrations (E_1, E_2)† the values in parenthesis are the standard deviation. The mean weighted (MeanPre-event) value between the two approximations was used in the analysis. Baseflow (Q_{base}) and Peakflow (Q_{peak}) are given where available.